

# BECC-engineered live-attenuated *Shigella* vaccine candidates display reduced endotoxicity with robust immunogenicity in mice

Robert Ernst

Rkernst@umaryland.edu

University of Maryland <https://orcid.org/0000-0001-5016-8694>

Matthew Sherman

University of Maryland, Baltimore <https://orcid.org/0000-0003-4918-6179>

Jane Michalski

University of Maryland School of Medicine

Sayan Das

University of Maryland <https://orcid.org/0000-0001-7445-2796>

Hyojik Yang

University of Maryland, Baltimore

Lakshmi Chandrasekaran

Walter Reed Army Institute of Research

Timothy O'Meara

Precision Vaccines Program <https://orcid.org/0000-0002-3651-5167>

David Dowling

Boston Children's Hospital <https://orcid.org/0000-0003-1095-6156>

Ofer Levy

Boston Children's Hospital <https://orcid.org/0000-0002-5859-1945>

Shoshana Barnoy

Walter Reed Army Institute of Research

Malabi Venkatesan

Walter Reed Army Institute of Research

---

## Article

**Keywords:** LPS, O-antigen, lipid A, BECC, endotoxicity, live-attenuated vaccine, TLR4, *Shigella*

**Posted Date:** June 11th, 2024

**DOI:** <https://doi.org/10.21203/rs.3.rs-4448907/v1>

**License:** © ⓘ This work is licensed under a Creative Commons Attribution 4.0 International License.

[Read Full License](#)

**Additional Declarations:** There is a conflict of interest OL is a consultant to GlaxoSmithKline (GSK) and Hillevax. OL and DJD are named inventors on patents held by Boston Children's Hospital regarding human in vitro systems that model vaccine action and small molecule vaccine adjuvants and are co-founders of Ovax, Inc. We, the authors, declare the following patents that are related to this manuscript: U.S. Patent No. 9,320,789 Issued: 26 Apr 2016 U.S. Patent Application No. 14/628,842 Filed: 23 February 2015 Title: Combinations of gene deletions for live attenuated shigella vaccine strains Inventors: Malabi Venkatesan, Ryan Ranallo, Shoshana Barnoy Owner: The United States of America, as represented by The Secretary Of The Army U.S. Patent No. 8,986,708 Issued: 24 Mar 2015 U.S. Patent Application No. 12/149,076 Filed: 23 February 2015 Title: Combinations of gene deletions for live attenuated shigella vaccine strains Inventors: Malabi Venkatesan, Ryan Ranallo, Shoshana Barnoy Owner: The United States of America, as represented by The Secretary Of The Army U.S. Patent No. 10,358,667 Issued: 23 Jul 2018 U.S. Patent Application No. 14/772,282 Filed: 02 Sept 2015 Title: Immunotherapeutic Potential of Modified Lipooligosaccharides/Lipid A Inventors: Robert K Ernst, Mark Pelletier, Adeline Hajjar Owner: The University of Maryland, Baltimore; Co-owned with Univ. of Washington, Seattle Status: Licensed to TollereBio Corporation. Optioned to Virtici, LLC U.S. Patent No. 11,124,815 Issued: 21 Sept 2021 U.S. Patent Application No. 16/431,536 Filed: 04 June 2019 Title: Immunotherapeutic Potential of Modified Lipooligosaccharides/Lipid A Inventors: Robert K Ernst, Mark Pelletier, Adeline Hajjar Owner: The University of Maryland, Baltimore; Co-owned with Univ. of Washington, Seattle Status: Licensed to TollereBio Corporation. Optioned to Virtici, LLC

---

1 **BECC-engineered live-attenuated *Shigella* vaccine candidates display reduced**  
2 **endotoxicity with robust immunogenicity in mice**

3  
4 Matthew E Sherman<sup>1</sup>, Jane Michalski<sup>1,2</sup>, Sayan Das<sup>1</sup>, Hyojik Yang<sup>1</sup>, Lakshmi Chandrasekaran<sup>3</sup>,  
5 Timothy R O’Meara<sup>4</sup>, David J Dowling<sup>4,5</sup>, Ofer Levy<sup>4,5,6</sup>, Shoshana Barnoy<sup>3</sup>, Malabi Venkatesan<sup>3</sup>,  
6 Robert K Ernst\*<sup>1</sup>

7  
8 <sup>1</sup>University of Maryland-Baltimore, Department of Microbial Pathogenesis, Baltimore, MD  
9 21201 USA

10 <sup>2</sup>University of Maryland School of Medicine, Institute for Genome Sciences, Baltimore, MD  
11 21201 USA

12 <sup>3</sup>Walter Reed Army Institute of Research, Department of Diarrheal Disease Research, Bacterial  
13 Disease Branch, Silver Spring, MD 20910 USA

14 <sup>4</sup>*Precision Vaccines Program*, Boston Children’s Hospital, Boston, MA 02115 USA

15 <sup>5</sup>Department of Pediatrics, Harvard Medical School, Boston, MA 02115 USA

16 <sup>6</sup>Broad Institute of MIT & Harvard, Cambridge, MA 02142 USA

17  
18 \*Correspondence: [rkernst@umaryland.edu](mailto:rkernst@umaryland.edu)

19 **Summary**

20 *Shigella spp.* infection contributes significantly to the global disease burden, primarily affecting  
21 young children in developing countries. Currently, there are no FDA-approved vaccines against  
22 *Shigella*, and the prevalence of antibiotic resistance is increasing, making therapeutic options  
23 limited. Live-attenuated vaccine strains WRSs2 (*S. sonnei*) and WRSf2G12 (*S. flexneri* 2a) are  
24 highly immunogenic, making them promising vaccine candidates, but possess an inflammatory  
25 lipid A structure on their lipopolysaccharide (LPS; also known as endotoxin). Here, we utilized  
26 bacterial enzymatic combinatorial chemistry (BECC) to ectopically express lipid A modifying  
27 enzymes in WRSs2 and WRSf2G12, as well as their respective wild-type strains, generating  
28 targeted lipid A modifications across the *Shigella* backgrounds. Dephosphorylation of lipid A,  
29 rather than deacylation, reduced LPS-induced TLR4 signaling *in vitro* and dampened endotoxic  
30 effects *in vivo*. These BECC-modified vaccine strains retained the phenotypic traits of their  
31 parental strains, such as invasion of epithelial cells and immunogenicity in mice without adverse  
32 endotoxicity. Overall, our observations suggest that BECC-engineered live attenuated vaccines  
33 are a promising approach to safe and effective *Shigella* vaccines.

34

35 **Keywords**

36 LPS, O-antigen, lipid A, BECC, endotoxicity, live-attenuated vaccine, TLR4, *Shigella*

## 37 **Introduction**

38 *Shigella* are Gram-negative bacteria known to cause diarrheal disease in humans through  
39 ingestion of contaminated food and water<sup>1-4</sup>. Of the four pathogenic *Shigella* species (*S. sonnei*,  
40 *S. flexneri*, *S. boydii*, and *S. dysenteriae*), *S. sonnei* (*Ss*) and *S. flexneri* (*Sf*) cause the majority of  
41 disease in industrialized and developing countries, respectively<sup>5</sup>. Shigellosis (*Shigella*-induced  
42 diarrhea) affects all age groups but particularly plagues young children as uncontrolled  
43 inflammation and severe dehydration can lead to growth abnormalities, seizure, and even  
44 death<sup>2,6-9</sup>. The clinical severity<sup>10,11</sup> and emergence of antibiotic resistance<sup>12,13</sup> have prompted  
45 the development of multiple *Shigella* vaccine candidates that are currently in preclinical and  
46 clinical phases<sup>4,14</sup>. However, to date, there is no FDA-licensed *Shigella* vaccine.

47  
48 Protection against shigellosis is serotype-specific<sup>4,5,14,15</sup>, implicating the O-antigen component  
49 of lipopolysaccharide (LPS) as being the critical antigen for vaccine development. Vaccine  
50 strategies to prevent shigellosis have included glycoconjugate vaccines where the O-antigen is  
51 conjugated to carrier adjuvants<sup>4,5,14-16</sup> or a complex comprising LPS and the invasion plasmid  
52 antigens (Ipa) called Invaplex<sup>17-19</sup>. Another longstanding strategy has been the development of  
53 live-attenuated *Shigella* strains where the O-antigen remains in its native context on the outer  
54 membrane<sup>4,5,14,15,20</sup>. Current live-attenuated vaccine candidates focus primarily on *S. sonnei* and  
55 *S. flexneri* serotype 2a, which are epidemiologically important *Shigella* strains<sup>21</sup> and whose O-  
56 antigen structures are well characterized<sup>15</sup>.

57

58 A key advantage of live-attenuated *Shigella* vaccines, which generally contain genetic mutations  
59 or deletions in virulence-associated genes<sup>5,14</sup>, is that they mimic a natural *Shigella* infection and,  
60 therefore, generate an immune response that protects against future infection. While these  
61 vaccines induce protective immune responses against virulent challenge in volunteer studies<sup>22</sup>,  
62 significant issues including adverse reactogenicity have slowed the progress toward a  
63 universally accepted safe and effective *Shigella* vaccine<sup>4,5,14</sup>. For this study, we used the live-  
64 attenuated vaccine candidates WRSs2 (*S. sonnei* strain) and WRSf2G12 (*S. flexneri* 2a strain),  
65 developed by Walter Reed Army Institute of Research (WRAIR), which are principally  
66 attenuated by deletion of *virG* (also known as *icsA*) thereby prohibiting intercellular spread but  
67 also contain deletions in genes encoding enterotoxins<sup>23-31</sup>. WRSs2 and WRSf2G12 are second-  
68 generation vaccines whose first-generation counterparts (WRSS1 and SC602, respectively) were  
69 highly immunogenic in adults and children during clinical trials, but substantial reactogenicity  
70 was observed at the moderate to high doses required to confer protective immunity<sup>22,32-38</sup>. To  
71 improve the safety of WRSs2 and WRSf2G12, we chose to target the highly immunostimulatory  
72 LPS molecule present on the bacterial membrane, which is thought to be a major contributor to  
73 these adverse effects.

74

75 LPS is a glycolipid present on the outer membrane of Gram-negative bacteria and is composed  
76 of three regions: the O-antigen, core oligosaccharide, and lipid A membrane anchor<sup>39,40</sup>. Innate  
77 immune cells can recognize the lipid A region of LPS and initiate cytokine production to alert  
78 the immune system to the presence of a bacterial invader<sup>41</sup>. This occurs through a series of  
79 accessory proteins that guide the binding of lipid A to the TLR4/MD-2 receptor on the surface of

80 innate immune cells to drive downstream signaling, such as the NF- $\kappa$ B pathway, and induce  
81 pro-inflammatory cytokine production<sup>42,43</sup>. The TLR4/MD-2 response is primarily driven by the  
82 structural features of lipid A, which vary across Gram-negative bacteria<sup>41,42,44,45</sup>. *Shigella*  
83 synthesizes a prototypical lipid A structure comprised of six acyl chains (hexa-acylated) and two  
84 terminal phosphates (bis-phosphorylated)<sup>41</sup>. This structure is a potent stimulator of TLR4/MD-  
85 2<sup>46</sup>, and the ensuing pro-inflammatory cytokine production likely contributes to the febrile  
86 symptoms observed upon oral ingestion of *Shigella* for vaccination. Thus, the  
87 immunostimulatory lipid A moiety was the primary target for detoxification.

88  
89 In this study, we employed bacterial enzymatic combinatorial chemistry (BECC)<sup>47</sup> to detoxify  
90 WRSs2 and WRSf2G12, as well as their respective wild-type strains. Lipid A modifying enzymes  
91 LpxE (1-position phosphatase from *Francisella*) and PagL (3-position deacylase from  
92 *Salmonella*) were ectopically expressed in the *Shigella* backgrounds. Targeted lipid A  
93 dephosphorylation (LpxE), deacylation (PagL), or execution of both modifications (Dual) was  
94 confirmed using MALDI-TOF MS. Lipid A dephosphorylation, rather than deacylation, effectively  
95 diminished LPS-induced pro-inflammatory immune signaling. Furthermore, deacylation  
96 combined with dephosphorylation did not further reduce LPS-mediated signaling. Due to this,  
97 only dephosphorylated lipid A mutants (LpxE-modified) were generated in WRSs2 and  
98 WRSf2G12, generating WRSs2E and WRSf2G12E. These strains had reduced LPS-mediated pro-  
99 inflammatory cytokine production *in vitro* and severely blunted endotoxemia *in vivo*, yet they  
100 remained as capable as their parental strains to invade epithelia and generate immunogenicity  
101 against their O-antigen. Altogether, we characterize two live-attenuated *Shigella* vaccine

102 candidates (WRSs2E and WRSf2G12E), altered only in their lipid A region, which are greatly  
103 detoxified without any consequence to phenotypic traits suggesting that such live-attenuated  
104 strains are a promising approach to develop a safe and effective *Shigella* vaccine.

105

## 106 **Results**

### 107 **Targeted lipid A modifications in *Shigella***

108 We initially utilized our BECC system to engineer targeted lipid A modifications (Fig 1) in *S.*  
109 *sonnei* Moseley and *S. flexneri* 2a 2457T, the wild-type (WT) strains upon which WRSs2 and  
110 WRSf2G12 were derived, respectively. Expression of the lipid A biosynthetic enzymes LpxE and  
111 PagL alone, or in combination (termed “Dual”), from the osmotically inducible pSEC10M  
112 plasmid resulted in targeted modification of the lipid A structure, which was confirmed via  
113 MALDI-TOF MS analysis (Fig S1A, B). Successful lipid A modification in WT strains prompted the  
114 expression of the individual enzymes in first-generation live-attenuated vaccine strains WRSS1  
115 and SC602. Similar to the WT strains, upon plasmid-based expression of BECC constructs, lipid A  
116 dephosphorylation and deacylation were observed in WRSS1 and SC602 by MALDI-TOF MS,  
117 respectively (Fig S1C, D). This suggested that targeted lipid A modifications could be achieved in  
118 both WT and genetically attenuated strains of *Shigella*.

119

120 We next assessed whether these targeted lipid A modifications affected the  
121 immunostimulatory capacity of *Shigella* LPS. Purified LPS from Moseley and 2457T was  
122 normalized to keto-deoxy-octanoate (Kdo), a conserved sugar within the core oligosaccharide,  
123 and used to stimulate NF- $\kappa$ B reporter cells. Stimulation with LpxE- and Dual-modified LPS



124 resulted in a pronounced reduction in NF- $\kappa$ B signaling compared to WT LPS, whereas  
125 stimulation with PagL-modified LPS generated comparable NF- $\kappa$ B signaling to that of WT LPS  
126 (Fig S2). This suggested that lipid A dephosphorylation, rather than deacylation, was the most  
127 promising modification for reduced endotoxicity, and therefore, only LpxE- and Dual-  
128 modifications were pursued for the remainder of the study.

129

130 To remove the need for ectopic plasmid expression of the lipid A modification enzymes, we  
131 utilized Tn7 transposition to integrate the *lpxE* and Dual gene cassettes into the chromosome of  
132 Moseley and 2457T. Second-generation vaccine strains WRSs2 and WRSf2G12 were also  
133 chromosomally integrated with *lpxE*; however, the Dual gene cassette could not be  
134 chromosomally integrated into these specific vaccine strains. Chromosomally integrated strains  
135 were utilized for the remainder of the study. Moseley and 2457T are designated with LpxE<sup>+</sup> or  
136 Dual to indicate what chromosomal integration they contain. Vaccine strains WRSs2 and  
137 WRSf2G12 chromosomally integrated with *lpxE* are designated as WRSs2E and WRSf2G12E,  
138 respectively.

139

140 Using MALDI-TOF MS, we confirmed that chromosomal expression of *lpxE* and Dual resulted in  
141 lipid A modification across the various *Shigella* backgrounds (Fig 2). Site-specificity of the  
142 modifications was confirmed via MALDI-TOF MS/MS using the FLAT<sup>n</sup> approach<sup>48</sup>. WT, LpxE-, and  
143 Dual-modified LPS each synthesized their expected base peaks at *m/z* 1797, 1717, and 1490,  
144 respectively (Fig S3A), which were selected as the precursor ions for fragmentation (Fig S3B,  
145 circled in red). The large cluster of spectral peaks at *m/z* less than 1490 represents cardiolipin

146 (Fig S3A), another phospholipid that resides in the outer leaflet along with lipid A. Spectral  
147 peaks representing fragments from the precursor ions (Fig S3B) were mapped to the proposed  
148 chemical structures of WT, LpxE-, and Dual-modified *Shigella* lipid A (Fig S3C). Determination of  
149 the location of the terminal phosphate modification at the 1-position was confirmed by the  
150 fragment ion still present at  $m/z$  690 in the LpxE-modified structure, and the deacylation  
151 modification at the 3-position was confirmed by the ions generated from the  $^{0,2}A_2$  cross-ring  
152 cleavage event (Fig S3C).

153

#### 154 **BECC-modified *Shigella* strains phenocopy their isogenic parental strains**

155 Live-attenuated *Shigella* strains have fundamental requirements that enable them to function  
156 as effective oral vaccines. First, large-scale production requires efficient growth in culture.  
157 Secondly, these strains must be capable of invading gut epithelia, a step during infection that  
158 elicits the host immune response required for mucosal immunity<sup>14</sup>. Lastly, host defense  
159 responses must be unaltered, such as the secretion of CXCL8 from the gut epithelia, which  
160 recruits polymorphonuclear leukocytes to the site of infection to clear the bacteria<sup>10</sup>. Thus, any  
161 limitation with respect to growth, invasion, or the host response would render our BECC-  
162 modified *Shigella* strains unsuitable to be used as vaccine candidates.

163

164 To evaluate the capacity to grow in culture, we assayed the growth kinetics of our BECC-  
165 modified *Shigella* and compared it to their isogenic parental strains. Over the course of 15  
166 hours, BECC-modified *Shigella* showed minimal growth alterations as compared to their

167 unmodified counterparts (Figure S4), suggesting BECC-modification had minimal impact on the  
168 capacity of the *Shigella* strains to grow *in vitro*.

169

170 To evaluate the invasion of epithelia by *Shigella* (intracellular bacterial burden recovered as a  
171 percentage of the inoculum), we employed a gentamicin protection assay<sup>26,28,29</sup>. The BECC-  
172 modified *S. sonnei* strains invaded similarly to their parental strains. As found previously<sup>26</sup>,  
173 WRSs2 strains invaded the epithelial cells significantly more than the Moseley strains (Fig 3A).  
174 For *S. flexneri 2a* strains, while LpxE-modification did not impact invasiveness, Dual-  
175 modification resulted in a significantly lower invasion than the WT (Fig 3B), likely due to a high  
176 frequency of invasion plasmid loss compared to the other *S. flexneri 2a* strains (data not  
177 shown). Beyond invasion, we also measured CXCL8 concentrations in the supernatant to assess  
178 the host response to infection with our BECC-modified *Shigella*, which showed the same  
179 pattern as invasion (Figure 3C, D). This suggested that, except for the Dual-modification in 257T,  
180 the targeted lipid A modifications did not impact the phenotypic traits of *Shigella*, such as  
181 growth, invasion of gut epithelia, or the host response to infection.

182

### 183 **Lipid A modifications reduced endotoxicity *in vitro* and *in vivo***

184 Since detoxification of *Shigella* lipid A was the primary objective of this study, we determined  
185 the level of endotoxicity using purified LPS from the chromosomally integrated strains. HEK-  
186 Blue cells stably expressing either the human or mouse orthologs of TLR4/MD-2/CD-14  
187 (hereafter referred to as “hTLR4” or “mTLR4”) and containing an NF- $\kappa$ B reporter were  
188 stimulated with Kdo normalized LPS from Moseley and 2457T. Stimulation with LpxE- and Dual-

189 modified LPS resulted in diminished NF- $\kappa$ B activation in both hTLR4 and mTLR4 reporter cell  
190 lines (Fig 4A). Similar results were observed in NF- $\kappa$ B reporter cell lines that endogenously  
191 expressed the human (THP-1 Dual) or mouse (RAW-Blue) orthologs of TLR4 and its coreceptors  
192 (Fig S5). Furthermore, stimulation with LPS from WRSs2E and WRSf2G12E displayed reduced  
193 NF- $\kappa$ B signaling compared to LPS from their respective parental strain (Fig S6). Altogether these  
194 data suggested that the potent pro-inflammatory cytokine production from WT *Shigella* LPS is  
195 greatly diminished upon LpxE-modification.

196  
197 To examine the cytokine profile from primary cells, we stimulated human peripheral blood  
198 monocytes (PBMCs) from 4 different study participants with the same panel of purified LPS  
199 molecules and measured the cytokine and chemokine concentrations in the supernatant by  
200 multiplex analysis. BECC-modified LPS induced a similar cytokine profile to WT LPS with CXCL8,  
201 IL-6, IFN $\gamma$ , IL-1 $\beta$ , TNF- $\alpha$ , and IL-10 present in decreasing abundance, respectively (Fig 4B). This  
202 pattern was conserved across the 4 participants and with LPS from WRSs2 and WRSf2G12 (Fig  
203 S7). Notably, production of these cytokines and chemokines was dampened upon stimulation  
204 with BECC-modified LPS, as compared to unmodified LPS from 2457T and WRSf2G12 (Fig S7A).  
205 Reduced cytokine and chemokine concentrations were comparable between LpxE- and Dual-  
206 modified 2457T LPS, which again suggested that dephosphorylation alone was sufficient to  
207 decrease pro-inflammatory cytokine production. Similarly, LpxE- and Dual-modified LPS from  
208 Moseley demonstrated reduced levels of cytokine and chemokine production; however, WT LPS  
209 from Moseley was less stimulatory than expected (Fig S7B). A separate experiment showed that  
210 LpxE- and Dual-modified LPS from Moseley demonstrated reduced induction of TNF- $\alpha$  from

211 PBMCs, and to a similar degree, compared to WT LPS (Fig S7C), which confirmed that  
212 dephosphorylated *Shigella* lipid A does indeed reduce pro-inflammatory cytokine production *in*  
213 *vitro* across all *Shigella* backgrounds.

214

215 To confirm that the BECC-modified LPS was also detoxified *in vivo*, we employed an acute  
216 murine endotoxicity study whereby a lethal dose of LPS was injected intraperitoneally into  
217 mice, and their health status was monitored over the course of 72 hours. Whereas injection of  
218 WT LPS from Moseley or 2457T was lethal by 24 hours post-injection, all mice receiving LpxE- or  
219 Dual-modified LPS survived after receiving the same dose (Fig 5A). The same pattern was  
220 observed using LPS from WRSs2 and WRSf2G12 (Fig 5B). Altogether, this data suggested that  
221 dephosphorylation of lipid A was sufficient to reduce endotoxicity *in vivo*.

222

### 223 **LpxE-modification did not compromise the immunogenicity of the *Shigella* vaccine strains**

224 To evaluate their potential use as vaccine candidates, we compared the immunological  
225 response of WRSs2E and WRSf2G12E to their parental strains in a mouse model. As mice do not  
226 experience diarrheal episodes from ingestion of *Shigella*, we evaluated vaccine efficacy through  
227 the generation of *Shigella*-specific immunological responses. Using three routes of vaccination  
228 (oral, intranasal, and intramuscular) and two different types of vaccines (live bacteria or  
229 purified LPS) (Fig S8A), we determined that intranasal administration of live bacteria at Day 0,  
230 14, and 28 (prime-boost-boost, respectively) generated the most reliable serum antibody  
231 response against serotype-specific LPS (Fig S8B). Using this intranasal approach and the same  
232 vaccination scheme of prime-boost-boost at Day 0, 14, and 28, respectively, we showed that

233 vaccination with WRSs2E or WRSf2G12E elicited strong serum IgG and IgA responses against  
234 serotype-specific LPS, that mimicked the response from their parental strains (Fig 6A, B).  
235 Although statistically significant differences in antibody titers were observed between the  
236 parental and LpxE-modified strains at specific time points, these differences did not remain  
237 throughout the entire vaccine study. At Day 56, four weeks after the final vaccine dose was  
238 delivered, the skewing of IgG subclasses 2a and 1 was similar for WRSs2E and WRSf2G12E  
239 compared to their parental strains (Fig 6C). The same patterns were observed in a second  
240 independent vaccine study (Fig S9). Ultimately, this data supports the notion that WRSs2E and  
241 WRSf2G12E promote a similar adaptive immune response as their parental strains.

242

243

## 244 **Discussion**

245 Despite significant advances in our understanding of *Shigella* pathogenesis and the  
246 development of many vaccine candidates<sup>49</sup>, to date, there is no FDA-licensed vaccine available.  
247 This study utilized second-generation vaccine candidates WRSs2 and WRSf2G12, whose first-  
248 generation strains were generally well tolerated in clinical trials but deemed too reactogenic to  
249 be considered safe for general use<sup>33,37</sup>. These second-generation vaccine strains contain a suite  
250 of genetic manipulations that remove known enterotoxins and reduce the spread of the  
251 bacterium across gut epithelia<sup>24,26,29</sup>. In this study, we describe the engineering and  
252 characterization of an additional modification, specifically the dephosphorylation of their lipid A  
253 structure, to generate WRSs2E and WRSf2G12E, which have reduced endotoxicity while  
254 retaining the same phenotypic traits as their isogenic parental strains.

255

256 The lipid A modifications engineered in this study utilized the BECC approach whereby prior  
257 identification of lipid A modifying enzymes from a variety of Gram-negative bacteria then  
258 enabled the expression of select enzymes within a bacterium of interest. Previously, the BECC  
259 system has been employed to generate custom-designed lipid A molecules in *Yersinia*<sup>50-56</sup>;  
260 however, this study extends its use to *Shigella* species, suggesting it is applicable to a variety of  
261 Gram-negative bacteria. More specifically, we showed that BECC enabled robust lipid A  
262 modification in both WT and vaccine strains of *Shigella*. Whereas multiple lipid A related  
263 spectral peaks were present upon plasmid-based expression of BECC constructs (Fig S1),  
264 chromosomal expression generated a single spectral peak (Fig 2) indicative of more complete  
265 lipid A modification on the outer membrane. This demonstrates a newfound approach for the

266 expression of BECC enzymes since here we showed that chromosomally expressing strains are  
267 both stable and robustly modify their lipid A, all without the requirement for antibiotic  
268 selection.

269  
270 Furthermore, to function as an effective oral vaccine, specific phenotypic requirements are  
271 required that may be altered upon engineering modified lipid A strains. We showed that  
272 dephosphorylation of lipid A had no impact on invasion or growth; however, Dual-modification  
273 (both dephosphorylation and deacylation) caused *S. flexneri* 2a 2457T to lose its invasion  
274 plasmid more frequently, likely a consequence of increased membrane stress. This is further  
275 supported by the inability to chromosomally integrate the Dual construct into WRSs2 or  
276 WRSf2G12, suggesting a limit to the degree to which lipid A can be modified in already  
277 genetically attenuated strains.

278  
279 Additionally, we showed that dephosphorylation at the 1-position via LpxE was sufficient to  
280 effectively blunt the LPS-induced pro-inflammatory response from both human and murine  
281 immune cells. This is analogous to other contexts, such as sepsis, where human alkaline  
282 phosphatase dephosphorylates LPS to reduce inflammatory signaling<sup>57</sup>. Traditionally, however,  
283 it is thought that deacylation of lipid A reduces LPS-induced signaling through TLR4/MD-2 as  
284 tetra- and penta-acylated structures are generally less immunostimulatory than hexa-  
285 acylated<sup>42</sup>. Here, we showed that PagL-mediated penta-acylated *Shigella* lipid A, lacking the 3-  
286 position backbone acyl chain, did not reduce LPS-mediated signaling (Fig S2). It has been shown  
287 that penta-acylated *Shigella* lipid A lacking an acyl chain at a different site has reduced LPS-



288 induced signaling. Rossi *et. al.*, showed that an *htrB* mutant in *S. sonnei*, whose lipid A lacks the  
289 secondary acyl chain at the 2'-position, displayed reduced TLR4 signaling in NF- $\kappa$ B reporter  
290 cells; however, the same mutation in *S. flexneri* 2a led to a compensatory C16:1 addition and no  
291 reduction in signaling compared to WT LPS<sup>46</sup>. This suggests that detoxification of *Shigella* lipid A  
292 via deacylation is site-specific. Furthermore, it emphasizes the complexity of achieving  
293 complete lipid A deacylation via genetic manipulation in *Shigella*. For instance, *Shigella* contains  
294 two *msbB* genes (both encoding MsbB/LpxM), one chromosomal and one on its invasion  
295 plasmid<sup>58,59</sup>. Additionally, *Shigella* can induce *lpxP* (encodes LpxP, C16:1 acylase) in the absence  
296 of *htrB* (encodes HtrB/LpxL) under stress-inducing conditions<sup>45,60,61</sup>. Altogether, this genetic  
297 redundancy of lipid A biosynthetic enzymes in *Shigella* highlights its drive to maintain hexa-  
298 acylated lipid A. Using BECC avoids this complication, as it introduces exogenous lipid A  
299 modifying enzymes and prevents induction of compensatory mechanisms that revert its lipid A  
300 back to the hexa-acylated state. This is emphasized in the present study as primarily a single  
301 spectral peak was observed in the MALDI-TOF MS spectra upon expression of BECC constructs  
302 across the various *Shigella* backgrounds (Fig 2), suggesting that the outer membrane contains  
303 predominantly the targeted lipid A structure without any compensatory lipid A modifications.  
304  
305 Despite remodeling of the lipid A region of LPS in the WRSs2E and WRSf2G12E, murine  
306 vaccination with these strains generated similar immune responses to their isogenic parental  
307 strains (Fig 6 and S9). This suggested that serotype-specific immunity in response to infection  
308 with these strains was unaffected by BECC modification. Since *Shigella* does not cause diarrheal  
309 disease upon ingestion in rodents, only immunological responses were evaluated in this study;

310 however, the first-generation variants of WRSs2 (WRSS1) and WRSf2G12 (SC602) have shown  
311 efficacy against shigellosis in humans<sup>22,36</sup>. Since LpxE-modification abrogates the toxic effects of  
312 LPS and does not appear to impact immunogenicity, this supports the notion that oral  
313 vaccination in humans with WRSs2E and WRSf2G12E would have reduced reactogenicity while  
314 maintaining robust immunogenicity and protection against shigellosis.

315

316 Overall, the need for a *Shigella* vaccine remains a priority. While it has been proposed that  
317 endemic *Shigella* can be controlled via public health efforts, the low infectious dose combined  
318 with its capacity to acquire extreme drug resistance has bolstered vaccination as a promising  
319 option to control the spread of this pathogen. To date, live-attenuated *Shigella* vaccines have  
320 shown immunological success in humans and, in some cases, protection against virulent  
321 challenges; this suggests that optimization of current live-attenuated vaccine candidates is a  
322 promising approach. A significant drawback with live-attenuated vaccine candidates, however,  
323 is the adverse effects from ingestion of high doses of bacteria containing the  
324 immunostimulatory hexa-acylated *Shigella* LPS. The BECC-modified vaccine strains of *Shigella*  
325 developed in this study, namely WRSs2E and WRSf2G12E, contain detoxified LPS and thus have  
326 promise to be better tolerated, safer, live-attenuated vaccine candidates.

327 **Acknowledgments**

328 We thank Dr. David Rasko for analyzing the genomic data to confirm the site-specific location of  
329 the chromosomal integration of BECC enzymes. RKE and MV would like to thank the  
330 Department of Defense Medical Research Program grant W81XWH1920025 for funding. JM  
331 would like to thank NIH/NIAID U19 AI110820 for funding.

332

333 **Author contributions**

334 M.E.S., J.M., L.C., S.B., M.V., and R.K.E. designed the study and participated in discussion and  
335 interpretation of the results. M.E.S., J.M., S. D., H. Y., S.B., L.C., and T.R.O. performed the  
336 experiments and data analysis. M.E.S executed the MS analysis and was the primary person  
337 who performed all *in vitro* and *in vivo* data. J.M. designed the constructs and established the  
338 molecular biology techniques. S.D. aided in executing the animal work. H.Y. performed the  
339 MS/MS analysis. S.B. and L.C. aided in strain characterization. T.R.O. assisted in the PBMC  
340 experiments under the supervision of D.J.D. and O.L. Lastly, M.E.S. wrote the manuscript and all  
341 authors revised the manuscript.

342

343 **Declaration of interests**

344 Material has been reviewed by the Walter Reed Army Institute of Research. There is no  
345 objection to its presentation and/or publication. The opinions or assertions contained herein  
346 are those of the authors, and do not necessarily reflect the official policy or position of the  
347 Department of the Army, Department of Defense, or the U.S. Government.

348

349 All animal research was conducted under an IACUC-approved animal use protocol in an AAALAC  
350 International - accredited facility with a Public Health Services Animal Welfare Assurance and in  
351 compliance with the Animal Welfare Act and other federal statutes and regulations relating to  
352 laboratory animals.

353

354 OL is a consultant to GlaxoSmithKline (GSK) and HilleVax. OL and DJD are named inventors on  
355 patents held by Boston Children's Hospital regarding human *in vitro* systems that model vaccine  
356 action and small molecule vaccine adjuvants and are co-founders of Ovax, Inc.

357

358 We, the authors, declare the following patents that are related to this manuscript:

359

360 U.S. Patent No. 9,320,789

361 Issued: 26 Apr 2016

362 U.S. Patent Application No. 14/628,842

363 Filed: 23 February 2015

364 Title: Combinations of gene deletions for live attenuated *shigella* vaccine strains

365 Inventors: Malabi Venkatesan, Ryan Ranallo, Shoshana Barnoy

366 Owner: The United States of America, as represented by The Secretary Of The Army

367

368 U.S. Patent No. 8,986,708

369 Issued: 24 Mar 2015

370 U.S. Patent Application No. 12/149,076  
371 Filed: 23 February 2015  
372 Title: Combinations of gene deletions for live attenuated *shigella* vaccine strains  
373 Inventors: Malabi Venkatesan, Ryan Ranallo, Shoshana Barnoy  
374 Owner: The United States of America, as represented by The Secretary Of The Army  
375  
376 U.S. Patent No. 10,358,667  
377 Issued: 23 Jul 2018  
378 U.S. Patent Application No. 14/772,282  
379 Filed: 02 Sept 2015  
380 Title: Immunotherapeutic Potential of Modified Lipooligosaccharides/Lipid A  
381 Inventors: Robert K Ernst, Mark Pelletier, Adeline Hajjar  
382 Owner: The University of Maryland, Baltimore; Co-owned with Univ. of Washington, Seattle  
383 Status: Licensed to TollereBio Corporation. Optioned to Virtici, LLC  
384  
385 U.S. Patent No. 11,124,815  
386 Issued: 21 Sept 2021  
387 U.S. Patent Application No. 16/431,536  
388 Filed: 04 June 2019  
389 Title: Immunotherapeutic Potential of Modified Lipooligosaccharides/Lipid A  
390 Inventors: Robert K Ernst, Mark Pelletier, Adeline Hajjar  
391 Owner: The University of Maryland, Baltimore; Co-owned with Univ. of Washington, Seattle

392 Status: Licensed to TollereBio Corporation. Optioned to Virtici, LLC

393

394 **Data availability statement**

395 The datasets generated during and analyzed during the current study are available from the

396 corresponding author on reasonable request.

397 **Figure Legends**

398 **Figure 1: Lipid A modifications generated by BECC constructs used in this study**

399 (A) The WT lipid A structure of *Shigella* along with the (B) LpxE- (C) PagL- and (D) Dual-modified  
400 resultant structures, lacking a phosphate, 3OH C14 acyl chain, or both, respectively. The  
401 expected  $m/z$  for the  $[M-H]^-$  ions observed in MALDI-TOF spectra are displayed for each  
402 structure.

403

404 **Figure 2: MALDI-TOF MS analysis of lipid A related peaks for BECC-modified *Shigella* strains**

405 Representative MALDI-TOF MS spectra for WT and vaccine strains of (A) *S. sonnei* and (B) *S.*  
406 *flexneri* 2a chromosomally expressing *lpxE* or Dual. Spectral peaks represent  $[M-H]^-$  ions.  
407 Colored peaks correspond to the expected structures detailed in Figure 1. Arrows depict the  
408 loss of a phosphate ( $HPO_3$ ) or acyl chain (3OH C14) from the indicated lipid A species.

409

410 **Figure 3: Invasion of epithelial cells by *Shigella* and corresponding CXCL8 production**

411 Invasion of HT29 cells after 4 hours of infection (MOI of 10) with (A) *S. sonnei* and (B) *S. flexneri*  
412 2a strains. CXCL8 production in the cell supernatant after the 4-hour infection with (C) *S. sonnei*  
413 and (D) *S. flexneri* 2a strains. Statistical significance determined by ordinary one-way ANOVA. \*  
414 and \*\*\* represent p-values of  $\leq 0.05$  and  $\leq 0.001$ , respectively.

415

416 **Figure 4: Stimulation of reporter and primary cells with Kdo normalized LPS from *Shigella***

417 (A) HEK-Blue cells stably expressing an NF- $\kappa$ B reporter under the control of the human and  
418 mouse orthologs of TLR4/MD-2/CD-14 (named hTLR4 or mTLR4, respectively) were stimulated

419 across 10-fold dilutions, in duplicate, of Kdo standardized LPS for 18 hours at 37°C with 5% CO<sub>2</sub>.  
420 LPS was purified from *S. sonnei* Moseley or *S. flexneri* 2a 2457T. (B) Representative cytokine  
421 profile from one PBMC donor, as measured by MSD multiplex, upon stimulation of the PBMCs  
422 with the aforementioned LPS at 1 pg/mL Kdo for 48 hours at 37°C with 5% CO<sub>2</sub>. Numbers in  
423 grey denote cytokine concentration in pg/mL.

424

425 **Figure 5: Assessment of the toxicity of *Shigella* LPS via a murine acute endotoxemia model**

426 Survival curves for mice (n=5) receiving a Kdo normalized dose of LPS intraperitoneally,  
427 representative of 15 mg/kg, using purified LPS from (A) WT strains and (B) vaccine strains of *S.*  
428 *sonnei* and *S. flexneri* 2a.

429

430 **Figure 6: Antibody titers from a *Shigella* murine vaccine study**

431 Serum IgG and IgA geometric mean titers against (A) *S. sonnei* Moseley LPS or (B) *S. flexneri* 2a  
432 2457T LPS for mice (n=15) vaccinated intranasally with 10<sup>6</sup> CFU at day 0, 14, and 28 as indicated  
433 by the arrows below the X-axis. (C) Serum IgG2a and IgG1 titers at day 56 against serotype-  
434 specific LPS. Statistical significance was determined by 2way ANOVA. \* and \*\*\*\* represent p-  
435 values of ≤ 0.05 and ≤ 0.0001, respectively.



436 **Methods**

437 **Ethics statement**

438 All animal procedures were approved by the University of Maryland, Baltimore Institutional  
439 Animal Care and Use Committee (IACUC #0222002). In all studies, female BALB/cJ mice (Jax  
440 Laboratories) were utilized. Mouse husbandry was conducted according to the procedures  
441 established at the University of Maryland, Baltimore.

442

443 **Bacterial strains and growth conditions**

444 Bacterial strains used in these studies are listed in Table S1. Bacteria were grown at 30°C or  
445 37°C in Lysogenic Broth (Teknova) and Tryptic Soy broth (TSB) or on Tryptic Soy agar (TSA)  
446 (Becton Dickinson) supplemented with 50 µg/mL neomycin (Sigma) or 60 µg/mL carbenicillin  
447 (Sigma) as needed. All strains were supplemented with 1 mM MgCl<sub>2</sub> to repress the PhoPQ two-  
448 component regulatory system. Growth curves were performed in a flat-bottom 96-well  
449 uncoated sterile plate (Costar) and recorded using a Cerillo Stratus instrument (Cerillo). Each  
450 well was inoculated with 10<sup>5</sup> CFU in 200 µL TSB and incubated with shaking (180 RPM), at 37°C  
451 for 15 hours. Absorbance readings at 600 nm were taken every 15 minutes.

452

453 **Molecular genetic techniques**

454 Standard DNA techniques, liquid media, and agar plates were used as described<sup>62</sup>. Restriction  
455 endonucleases and T4 DNA ligase were used as recommended by the manufacturer (New  
456 England Biolabs). DNA used for cloning purposes was PCR amplified using 10mM dNTP mix  
457 (Thermo Scientific) and high-fidelity DNA polymerases Q5 (New England Biolabs) or Pfu ultra II

458 fusion HS (Agilent) according to manufacturer's instructions. Go-Taq polymerase (Promega) was  
459 used for genetic screening. DNA oligonucleotides were obtained from Integrated DNA  
460 Technologies and are listed in Table S2. All plasmid constructs (Table S3) were confirmed by  
461 double-stranded sequencing (Azenta) and maintained in *E. coli* DH5 $\alpha$  or *E. coli* TOP10  
462 (ThermoFisher).

463

#### 464 **Generation of plasmid-based BECC-modified *Shigella* strains**

465 LPS modifying enzymes LpxE, PagL, and LpxE-PagL in tandem (termed "Dual") were first cloned  
466 and expressed in pSEC10<sup>63</sup> under the osmotically controlled *E. coli ompC* promoter ( $P_{ompC}$ ). A  
467 codon-optimized form of *lpxE* from *Francisella novicida* was synthesized by GenScript and  
468 cloned into pUC57, yielding pUC57::*lpxE*. The 720 bp *lpxE* gene was amplified by PCR from  
469 pUC57::*lpxE* using Q5 polymerase (New England Biolabs) and primer set *lpxE-F/lpxE-R*, trimmed  
470 with restriction enzymes BamHI and NheI, and ligated into the BamHI/NheI site of pSEC10  
471 resulting in the construct pSEC10:: $P_{ompC}$ -*lpxE*. The *pagL* gene was amplified by PCR from  
472 *Salmonella minnesota* (Genbank accession AE006468.2) using Q5 polymerase and primer set  
473 *pagL-F/pagL-R*. A 570 bp amplicon was trimmed with BamHI/NheI and ligated into the 6630 bp  
474 BamHI/NheI digested fragment of pSEC10 yielding pSEC10:: $P_{ompC}$ -*pagL*. Both *lpxE* and *pagL*,  
475 each preceded by a ribosomal binding site, were synthesized in tandem behind  $P_{ompC}$  and  
476 cloned into vector pUC57K by GenScript yielding pUC57K:: $P_{ompC}$ -Dual. The initial subcloning of  
477 *pagL* into pSEC10 included six additional bps (GTGTAT) that encoded an alternative start codon  
478 present in the *S. minnesota* sequence; this 6 bp sequence was not included in the Dual  
479 construct. The  $P_{ompC}$ -Dual gene cassette was then cloned into a modified version of pSEC10

480 (pSEC10M). Briefly, primer set pSEC10M-F/pSEC10M-R was self-annealed, trimmed with  
481 EcoRI/NheI, and ligated into a 5775 bp gel purified EcoRI/NheI digested pSEC10 and  
482 transformed into *E. coli* TOP10. The resulting pSEC10M had a multiple cloning site [EcoRI-NotI-  
483 SwaI-NheI] in place of the *ompC* promoter and *clyA* gene. The 1.9 kb SwaI  $P_{ompC}$ -Dual gene  
484 cassette isolated from pUC57K:: $P_{ompC}$ -Dual was ligated into the SwaI digested site of pSEC10M  
485 and transformed into *E. coli* TOP10 yielding construct pSEC10M:: $P_{ompC}$ -Dual. Plasmids  
486 pSEC10:: $P_{ompC}$ -*lpxE*, pSEC10:: $P_{ompC}$ -*pagL*, and pSEC10M:: $P_{ompC}$ -Dual were electroporated into the  
487 wild-type strains of *S. sonnei* and *S. flexneri* 2a and selected on TSA with neomycin. Successful  
488 transformants were used to inoculate a 2 mL overnight culture in TSB with neomycin, which  
489 received a final concentration of 15% glycerol, followed by storage at -80°C.

490

#### 491 **Generation of *attTn7* chromosomally integrated BECC-modified *Shigella* strains**

492 We mobilized  $P_{ompC}$ -*lpxE* and  $P_{ompC}$ -Dual into the *Shigella* chromosome *attTn7* site using a site-  
493 specific insertion method utilizing the Tn7 recombination machinery on a temperature-sensitive  
494 plasmid pGRG36<sup>64</sup>. A 1225 bp amplicon of the  $P_{ompC}$ -*lpxE* gene cassette was generated using  
495 template pSEC10:: $P_{ompC}$ -*lpxE*, Q5 polymerase (New England Biolabs) and primer set  $P_{ompC}$ -  
496 F/*lpxE*-R. This was then blunt-ligated into the SmaI digested site of pGRG36, yielding  
497 pGRG36:: $P_{ompC}$ -*lpxE*. A 1.9 kb  $P_{ompC}$ -Dual gene cassette flanked by SwaI restriction sites was  
498 isolated from pUC57K:: $P_{ompC}$ -Dual and ligated into the SmaI site of pGRG36 yielding  
499 pGRG36:: $P_{ompC}$ -Dual. The resulting pGRG36 construct was transformed into *E. coli* S17-1 and  
500 introduced into wild-type and 2<sup>nd</sup> generation vaccine strains of *S. sonnei* and *S. flexneri* 2a by  
501 conjugal mating. Briefly, 2 mL cultures were grown overnight. *E. coli* S17-1 plasmid

502 transformants were grown in the presence of carbenicillin at 30°C whereas *Shigella* cultures  
503 were grown without antibiotic at 37°C. Filter matings were performed by mixing 100 µL of  
504 *Shigella* with 50 µL of *E. coli* S17-1 plasmid transformants, concentrated by centrifugation (8k x  
505 g for 1 minute), resuspended in 200 µL TSB, spread onto a 0.45 µM nylon filter (MSI Magna  
506 nylon 66) placed on the center of a TSA plate, and incubated for 5 hours at 30°C. Bacteria on  
507 the nylon filter were then resuspended in 1 mL TSB and plated onto TSA containing 0.01%  
508 Congo red dye (Sigma- Aldrich), carbenicillin, and 1 mM MgCl<sub>2</sub> and incubated overnight at 30°C.  
509 *Shigella* conjugants that grew at 30°C and were carbenicillin resistant were screened by PCR for  
510 the presence of *lpxE* and the *Shigella* invasion plasmid using GoTaq (Promega), and primer sets  
511 *lpxE-F/lpxE-R* (*lpxE*) and *ospD3-F/ospD3-R* (*ospD3*) or *lpxE-F/lpxE-R* (*lpxE*) and *ipaB-F/ipaB-R*  
512 (*ipaB*) for WT and vaccine strains, respectively. Bacteria were plated on TSA containing 0.1%  
513 arabinose and incubated at 42°C overnight to promote Tn7 recombination and simultaneous  
514 curing of pGRG36. Isolates that were carbenicillin sensitive and Congo Red positive, were  
515 assayed by PCR for the presence of *lpxE* using primer set *lpxE-F/lpxE-R* and for the *Shigella*  
516 invasion plasmid using *ospD3* primer set *ospD3-F/ospD3-R* or *ipaB* primer set *ipaB-F/ipaB-R* for  
517 WT and vaccine strains, respectively. Confirmed integrants were stored in 15% glycerol at -80°C.  
518 Bacterial genomes were sequenced at the Microbial Genome Sequencing Center (SeqCenter)  
519 and analyzed using the RAST software<sup>65</sup> which confirmed the insertion of the gene cassettes  
520 into the *attTn7* site.

521

522 **MALDI-TOF MS and MS/MS analysis of lipid A**

523 Functional screening of *Shigella* strains to confirm lipid A modification was performed using the  
524 Fast Lipid Analysis Technique (FLAT) coupled to MALDI-TOF MS analysis<sup>66</sup>. Briefly, a single  
525 colony was spotted on a MALDI plate and overlaid with 1  $\mu$ L of citrate buffer (200 mM citric  
526 acid, 100 mM trisodium citrate, pH 3.5). The plate was incubated in a humidified, closed, glass  
527 chamber for 30 minutes at 110°C, cooled, washed with endotoxin-free water, and 1  $\mu$ L of 10  
528 mg/mL norharmane matrix (Sigma-Aldrich) dissolved in chloroform : methanol (2:1 v/v) was  
529 spotted onto the samples on the MALDI plate. MALDI-TOF MS analysis was performed using a  
530 Bruker Microflex LRF equipped with a 337 nm nitrogen laser. Spectra were acquired in the  
531 negative ion and reflectron mode. Analyses were conducted at < 60% global intensity with 300  
532 laser shots for each spectrum acquisition. Spectra were recorded in triplicate. Agilent ESI tune  
533 mix (Agilent) was used for mass calibration. FlexAnalysis software version 3.4 (Bruker) was used  
534 to process the mass spectra with smoothed and baseline corrections. Further structural lipid A  
535 characterization was conducted by tandem mass spectrometry (MS/MS) analysis using the  
536 FLAT<sup>n</sup> procedure<sup>48</sup>. The FLAT process above was repeated, except the colony spotted onto an  
537 indium tin oxide (ITO) slide instead of a MALDI plate. MS/MS analysis was performed using a  
538 Bruker MALDI trapped ion mobility spectrometry Time-of-Flight (timsTOF) mass spectrometer  
539 equipped with a dual ESI/MALDI source with a SmartBeam 3D 10 KHz frequency tripled 355 nm  
540 Nd:YAG laser. The system was operated in “qTOF” mode (tims deactivated). Ion transfer tuning  
541 used the following parameters: Funnel 1 RF: 440.0 Vpp, Funnel 2 RF: 490.0 Vpp, Multipole RF  
542 490.0 Vpp, is CID Energy: 0.0 eV, and Deflection Delta: -60.0 V. The quadrupole used the  
543 following values for MS mode: Ion Energy: 4.0 eV and Low Mass 700.00 m/z. Collision cell

544 activation of ions used the following values for MS mode: Collision Energy: 9.0 eV and Collision  
545 RF: 3900.0 Vpp. The precursor ion was chosen by inputting targeted  $m/z$  values including two  
546 digits beyond the decimal point. Typical isolation width and collision energy were set to 4 – 6  
547  $m/z$  and 100 – 110 eV, respectively. Focus Pre-TOF used the following values: Transfer time  
548 110.0  $\mu\text{s}$  and Pre pulse storage 9.0  $\mu\text{s}$ . Agilent ESI Tune Mix (Agilent) was used to perform  
549 calibration. MALDI parameters in qTOF mode were optimized to maximize intensity by tuning  
550 ion optics, laser intensity, and laser focus. All spectra were collected at a laser diameter of 104  
551  $\mu\text{m}$  with beam scan on using 800 laser shots per spot using either 70% or 80% laser power.  
552 MS/MS data were collected in negative ion mode. In all cases, a matrix of 10 mg/mL  
553 norharmane dissolved in chloroform : methanol (2:1 v/v) was used. mMass software version  
554 5.5.0<sup>67</sup> was used to process the mass spectra with smoothed and baseline corrections.  
555 Identification of all fragment ions were determined based on ChemDraw Ultra version 10.0.

556

### 557 **LPS extraction and purification**

558 LPS was isolated using the double hot phenol method. Briefly, two liters of bacterial culture  
559 were harvested by centrifugation and resuspended in 90% phenol : endotoxin-free water (1:1  
560 v/v) and incubated at 65°C for 1 hour. After centrifugation, the aqueous phase was isolated  
561 from the two-phase solution (repeated three times total and pooled) and dialyzed for 36 hours  
562 against deionized water using pre-treated 1 kD MWCO RC tubing (Spectrumlabs.com), followed  
563 by flash freezing and lyophilization. The lyophilized product was resuspended in 20 mM Tris-HCl  
564 pH 8.4 supplemented with 2 mM  $\text{MgCl}_2$  and digested using 500 units of Benzonase and 100  
565  $\mu\text{g/mL}$  Dnase I for 2 hours at 37°C. The pH was subsequently adjusted to 7.4 using 1 N HCl and

566 the solution further digested with 100 µg/mL Proteinase K for 2 hours at 37°C. Water-saturated  
567 phenol was added, vortexed, and centrifuged (8,000 x g), and the upper aqueous phase was  
568 collected, dialyzed, and lyophilized. Further isolation of LPS was performed by serial washes in  
569 chloroform : methanol (2:1 v/v) as described<sup>68</sup>. The LPS was separated from contaminating  
570 lipoproteins as described<sup>69</sup> by resuspension in 0.2% TEA (triethylamine) and 0.5% DOC  
571 (deoxycholate), followed by the addition of 37°C water-saturated phenol and the upper  
572 aqueous phase collected. Finally, the LPS product was precipitated by the addition of cold 100%  
573 ethanol and 30 mM sodium acetate followed by incubation for 18 hours at -20°C. The LPS  
574 precipitate was harvested by centrifugation (5,000 x g, 20 minutes), washed in cold 100%  
575 ethanol, resuspended in endotoxin-free water (Quality Biological), and lyophilized.

576

#### 577 **Kdo assay for LPS quantification**

578 2-keto-3-deoxyoctonate (Kdo) standards ranging from 12 – 48 µg/mL in endotoxin-free water  
579 and 1 mg/mL LPS solution solutions were hydrolyzed in 0.018 N sulfuric acid (H<sub>2</sub>SO<sub>4</sub>) at 100°C  
580 for 20 minutes, followed by the addition of 25 µL of 9.1 mg/mL periodic acid (H<sub>5</sub>IO<sub>6</sub>) in 0.125 N  
581 H<sub>2</sub>SO<sub>4</sub> and incubation in the dark for 20 minutes. Samples then received 50 µL of 2.6% sodium  
582 arsenite (NaAsO<sub>2</sub>) in 0.5 N HCl was followed by the addition of 250 µL of 0.3% thiobarbituric  
583 acid (TBA). Samples were heated at 100°C for 10 minutes, quickly followed by the addition of  
584 125 µL of dimethyl sulfoxide (DMSO), and the measurement of absorbance at 550 nm. The  
585 absolute quantification is based on the interpolation of the standard curve provided by the  
586 Kdo<sub>2</sub> quantity. Half of the Kdo<sub>2</sub> quantity, representing Kdo<sub>1</sub> (referred to as simply “Kdo” in this  
587 study), was utilized for normalization.

588 **Murine acute endotoxemia**

589 LPS solutions of 45 µg/mL Kdo<sub>2</sub> (representative of 15 mg/kg if using dry weight instead) were  
590 prepared in sterile, endotoxin-free PBS (Quality Biology). LPS solutions were transferred to  
591 arbitrarily labeled tubes by a third-party observer to ensure blinding to group identifications  
592 and avoid bias in clinical score designations. Each mice received 100 µL of LPS solution using a  
593 slip tip 1 mL syringe attached to a 27-gauge ½ inch needle (Becton Dickinson) via the  
594 intraperitoneal route. Mice were monitored for 72 hours post-injection, receiving a clinical  
595 score/mouse based on appearance and mobility as described in Table S4. A clinical score of 5  
596 required euthanization as a consequence of no movement, noticeable stress, and an inability to  
597 return upright if placed on their side.

598

599 **Cell culture media and conditions**

600 RPMI-1640 (Gibco) complemented with 25 mM HEPES, 2 mM glutamine, 10% FBS, and 1%  
601 penicillin-streptomycin, referred to as cRPMI, was filter sterilized through a 0.22 µM filter flask  
602 and used for the THP-1 NF-κB-SEAP reporter cell line (THP-1 Dual, Invitrogen). DMEM (Corning)  
603 complemented with 3.7 g/L sodium bicarbonate, 2 mM glutamine, 10% FBS, and 1% penicillin-  
604 streptomycin, referred to as cDMEM, was filter sterilized through a 0.22 µM filter flask and  
605 used for the HT29 cells (courtesy of Dr. Eileen Barry, UMB), mTLR4/hTLR4 HEK-Blue cells  
606 (Invitrogen), and RAW-Blue cells (Invitrogen). All cells were maintained at 37°C with 5% CO<sub>2</sub>.

607

608



609 **NF- $\kappa$ B reporter cell line stimulations**

610 Sterile, cell culture-treated, 96-well flat bottom plates (Costar) were seeded with HEK-Blue,  
611 RAW-Blue, or THP-1 Dual reporter cells at  $6 \times 10^4$  cells/well. THP-1 cells received 100 ng/mL of  
612 vitamin D<sub>3</sub> (Sigma) prior to seeding in wells to enable cell differentiation. Cells were incubated  
613 for 18 hours at 37°C with 5% CO<sub>2</sub>, except the THP-1 cells, which were incubated for 72 hours to  
614 enable differentiation into monocyte-derived macrophages. Five 10-fold dilutions of Kdo  
615 standardized LPS ranging from 10<sup>2</sup> pg/mL to 10<sup>-2</sup> pg/mL was used to stimulate NF- $\kappa$ B  
616 production in cells. Cells were incubated at 37°C with 5% CO<sub>2</sub> for 18 hours. Detection of NF- $\kappa$ B  
617 was quantified using the Quanti-Blue (QB) reagent prepared according to the manufacturer's  
618 protocols (Invitrogen). The percent of relative NF- $\kappa$ B activation was normalized to the  
619 maximum OD 630 nm measured. Points were plotted as the mean  $\pm$  standard deviation of the  
620 relative NF- $\kappa$ B activation at each concentration using GraphPad Prism version 9 and fitted using  
621 a nonlinear regression of the log(agonist) versus response (three parameters).

622

623 **Stimulation of primary peripheral blood monocytes**

624 Human peripheral blood was collected from healthy adult study participants 18–40 years of age  
625 per a Boston Children's IRB-approved protocol (protocol number X07-05-0223). All participants  
626 signed an informed consent form prior to enrollment. Heparinized whole blood was centrifuged  
627 (500 x g, 10 minutes) prior to removal of the upper layer of platelet-rich plasma. The plasma  
628 was centrifuged (3,000 x g, 10 minutes) and platelet-poor plasma (PPP) was collected and  
629 stored on ice. The remaining blood was reconstituted to its original volume with heparinized  
630 Dulbecco's PBS and layered on Ficoll-Paque gradients (Cytiva) in Accuspin tubes (Sigma-Aldrich).

631 PBMCs were collected after centrifugation, washed twice with PBS, and seeded at  $2 \times 10^5$   
632 cells/well in 96-well U-bottom plates (Corning) in RPMI-1640 media (Gibco) supplemented with  
633 10% autologous PPP, 100 IU/ mL penicillin, 100  $\mu$ g/mL streptomycin, and 2 mM L-glutamine.  
634 PBMCs were incubated with 1 pg/mL Kdo standardized LPS for 24 hours at 37 °C with 5% CO<sub>2</sub>.  
635 The supernatants were recovered after centrifugation (500 x g, 5 minutes) and analyzed for  
636 TNF- $\alpha$  quantification.

637

638 For multiplex analysis, frozen PBMCs from 4 independent human donors were instead obtained  
639 from AllCells, snap-thawed, washed twice with warm cRPMI, and seeded at  $5 \times 10^5$  cells/well in  
640 96-well, sterile, uncoated U-bottom plates (Costar). PBMCs were incubated with 1 pg/mL Kdo  
641 standardized LPS for 48 hours at 37 °C with 5% CO<sub>2</sub>. The supernatants were recovered after  
642 centrifugation (400 x g, 5 minutes) and stored at -20°C until analyzed by MSD multiplex.

643

#### 644 **Invasion assays**

645 HT29 cells were seeded at a density of  $5 \times 10^5$  cells/well in 24-well flat bottom sterile plates  
646 (Corning) and incubated at 37°C for 18 hours with 5% CO<sub>2</sub>. *Shigella* cultures from overnight  
647 growth on TSA containing 0.01% Congo Red were used to generate a resuspension in sterile PBS  
648 pH 7.4. Inoculums of  $5 \times 10^6$  CFU were used to infect, giving an MOI of 10. Enumeration of the  
649 inoculation was confirmed in duplicate by plate counts on TSA. Bacteria were added to media-  
650 free, PBS-washed cell monolayers and the plates were centrifuged (3,000 x g, 5 minutes). After  
651 incubation for 90 minutes at 37°C with 5% CO<sub>2</sub>, cell monolayers were twice washed with sterile  
652 PBS, followed by the addition of cDMEM containing 50  $\mu$ g/mL gentamycin (Sigma-Aldrich) and

653 incubation for 2.5 hours. Supernatants were isolated and processed for human CXCL8 secretion  
654 by cytokine ELISA. The cell monolayer was twice washed with sterile PBS and lysed with 1%  
655 Triton X-100 (Sigma-Aldrich) in sterile PBS for 10 minutes at room temperature. Serial dilutions  
656 were plated in duplicate on TSA and incubated overnight at 37°C. The percentage of invasion  
657 was determined as the CFU/mL recovered normalized to the CFU/mL inoculated.

658

### 659 **Cytokine ELISA**

660 Cytokine analysis of host cell culture supernatants was performed using DuoSet ELISA kits (R&D  
661 Systems) according to the manufacturer's protocol. Briefly, plates were coated overnight at 4°C  
662 by adding 100 µL/well of 2 µg/mL capture antibody in ELISA coating buffer, washed three times  
663 PBS + 0.02% Tween-20 (PBST) and blocked with 300 µL/well 1% BSA in PBS for 1 hour at room  
664 temperature followed by three washes with PBST. Cell culture supernatants were diluted to  
665 reach a signal within the dynamic range. Bound cytokines were labeled by adding biotin-  
666 conjugated antibodies in block buffer (100 µL/well of 2 pg/mL) and incubated at room  
667 temperature for 2 hours. Plates were washed with PBST and incubated for 20 minutes with  
668 secondary antibody streptavidin-HRP, followed by the addition of a color substrate. The plates  
669 were read at both 450 nm and 562 nm and the difference taken as the final reading. The  
670 amount of cytokine is reported as picograms per mL of cell culture supernatant.

671

### 672 **Murine vaccination with live-attenuated *Shigella***

673 *Shigella* vaccine strains were grown at 37°C overnight on TSA containing 0.1% Congo Red. For  
674 intranasal vaccination, inoculums of  $3.33 \times 10^8$  CFU/mL and  $3.33 \times 10^7$  CFU/mL of *Shigella* were

675 prepared in sterile PBS and kept at room temperature. Mice were anesthetized using a Matrix  
676 VIP 3000 vaporizer (Midmark Animal Health) with isoflurane (Fluriso, VetOne): oxygen (Airgas,  
677 OX USPEAWBDS) mixture (1:1 mixing) for 1-2 minutes and 15  $\mu$ L of the vaccine inoculum was  
678 delivered to each nare (30  $\mu$ L in total) using a pipette. For oral gastric vaccination, inoculums of  
679  $1 \times 10^8$  CFU/mL and  $1 \times 10^7$  CFU/mL of *Shigella* were prepared in sterile PBS and kept at room  
680 temperature. Inoculums of 100  $\mu$ L were delivered by intra-gastric gavage using a 2-inch-long  
681 plastic feeding needle (VWR) connected to a 1 mL syringe (Becton Dickinson). For both  
682 vaccination methods, mice were monitored for adverse reactions post-immunization.  
683 Enumeration of the vaccine inoculums was determined by plate counts on TSA.

684

#### 685 **Murine vaccination with purified LPS**

686 Purified LPS from wild-type *S. sonnei* Moseley was obtained as described above (see LPS  
687 extraction and purification). For intranasal vaccination, solutions containing purified LPS at 1  
688 mg/mL and 0.66 mg/mL, dissolved in sterile PBS, were delivered intranasally as described  
689 above. For intramuscular vaccination, solutions containing purified LPS at 0.6 mg/mL and 0.4  
690 mg/mL, dissolved in sterile PBS, were prepared and stored at room temperature. Mice were  
691 immobilized using a restrainer, and 50  $\mu$ L of the solution was injected using a 1 mL syringe  
692 (Becton Dickinson) into the caudal muscle after disinfecting the area with 70% ethanol. For  
693 both vaccination methods, mice were monitored for adverse reactions post-immunization.

694

695

696

697 **Sera collection**

698 Mice were bled via the lateral saphenous vein using petroleum jelly and 27-gauge needles.

699 Blood was collected in a microvette 200 Z-gel tubes (Sarstedt), and the sera were isolated by

700 centrifugation (10,000 x g, 3 minutes) and stored in sealed uncoated 96-well flat bottom plates

701 (Thermo Fischer) at -20°C.

702

703 **Enzyme-linked immunosorbent assay (ELISA)**

704 Coating antigens used in ELISAs included purified LPS from wild-type *S. sonnei* Moseley or *S.*

705 *flexneri* 2a 2457T. Nunc MaxiSorp plates (ThermoFischer) were coated with 5 µg/mL serotype-

706 specific LPS in 100 mM carbonate coating buffer pH 9.6 (sodium bicarbonate/carbonate) and

707 incubated for 3 hours at 37°C. Plates were washed with PBS containing 0.05% Tween-20 (Sigma)

708 (PBST) and blocked with 10% non-fat dry milk powder (Quality Biological) in PBST overnight at

709 4°C. Sera was diluted in 5-fold increments starting with a 1:50 dilution in PBST, added to the

710 LPS-coated plates, and incubated at 37°C for 2 hours. Plates were washed with PBST. Incubation

711 for 1 hour with secondary HRP-conjugated antibodies, goat anti-mouse IgG, IgG1, IgG2a

712 (Southern Biotech) or goat anti-mouse IgA (Invitrogen) was followed by a 15 minute room

713 temperature incubation with 3,3',5,5'-tetramethylbenzidine (TMB) substrate (BD biosciences)

714 prepared according to manufacturer's protocol. KPL TMB stop solution (Sera Care) containing

715 1% HCl was added to each well, and the absorbance read at 450 nm. The endpoint titer was

716 determined as the absorbance reading that was equal to the reciprocal dilution required for the

717 signal to match the average blank (PBST alone, no sera). Samples were run in duplicate. Sera

718 from days 28, 42, and 56 of the vaccine study required dilutions of 1:1250 for IgG and IgG1  
719 titers and 1:250 for IgG2a to reach specific endpoints.

720

721 **Multiplex cytokine analysis**

722 MSD (Meso Scale Development) V-PLEX human proinflammatory panel 1 (10-plex) was used for  
723 the analysis of the human orthologs of IFN $\gamma$ , IL-1 $\beta$ , IL-2, IL-4, IL-6, CXCL8, IL-10, IL-12p70, IL-13  
724 and TNF $\alpha$  from 25  $\mu$ L of 6-fold dilutions of the supernatant from the stimulation of human  
725 PBMCs. Samples and calibrators were incubated at room temperature, shaking (500 RPM), for 2  
726 hours. Plates were washed with PBST and MSD detection antibody solution, prepared according  
727 to the manufacturer's protocol, was added and incubated shaking (500 RPM) at room  
728 temperature for 2 hours. Plates were washed with 150  $\mu$ L/well PBST followed by the addition of  
729 150  $\mu$ L/well of read buffer T. Plates were immediately read on an MSD SQ 120/120MM  
730 instrument. Cytokine concentration was determined by interpolation from a standard curve  
731 generated using the provided calibrators.

732

733 **References**

734 1 Vos, T. *et al.* Global, regional, and national incidence, prevalence, and years lived with  
735 disability for 310 diseases and injuries, 1990–2015: a systematic analysis for the Global  
736 Burden of Disease Study 2015. *The Lancet* **388**, 1545-1602 (2016).  
737 [https://doi.org:10.1016/s0140-6736\(16\)31678-6](https://doi.org:10.1016/s0140-6736(16)31678-6)

738 2 Wang, H. *et al.* Global, regional, and national life expectancy, all-cause mortality, and  
739 cause-specific mortality for 249 causes of death, 1980–2015: a systematic analysis for  
740 the Global Burden of Disease Study 2015. *The Lancet* **388**, 1459-1544 (2016).  
741 [https://doi.org:10.1016/s0140-6736\(16\)31012-1](https://doi.org:10.1016/s0140-6736(16)31012-1)

742 3 Troeger, C. *et al.* Estimates of the global, regional, and national morbidity, mortality, and  
743 aetiologies of diarrhoea in 195 countries: a systematic analysis for the Global Burden of  
744 Disease Study 2016. *The Lancet Infectious Diseases* **18**, 1211-1228 (2018).  
745 [https://doi.org:10.1016/s1473-3099\(18\)30362-1](https://doi.org:10.1016/s1473-3099(18)30362-1)

746 4 Walker, R. *et al.* Vaccines for Protecting Infants from Bacterial Causes of Diarrheal  
747 Disease. *Microorganisms* **9**, 1382 (2021).  
748 <https://doi.org:10.3390/microorganisms9071382>

749 5 Pasetti, M. F., Venkatesan, M. M. & Barry, E. M. in *Mucosal Vaccines* Ch. 30, 515-536  
750 (2020).

751 6 Liu, J. *et al.* Use of quantitative molecular diagnostic methods to identify causes of  
752 diarrhoea in children: a reanalysis of the GEMS case-control study. *The Lancet* **388**,  
753 1291-1301 (2016). [https://doi.org:10.1016/s0140-6736\(16\)31529-x](https://doi.org:10.1016/s0140-6736(16)31529-x)

754 7 Khalil, I. A. *et al.* Morbidity and mortality due to shigella and enterotoxigenic Escherichia  
755 coli diarrhoea: the Global Burden of Disease Study 1990–2016. *The Lancet Infectious*  
756 *Diseases* **18**, 1229-1240 (2018). [https://doi.org:10.1016/s1473-3099\(18\)30475-4](https://doi.org:10.1016/s1473-3099(18)30475-4)

757 8 Williams, P. C. M. & Berkley, J. A. Guidelines for the treatment of dysentery (shigellosis):  
758 a systematic review of the evidence. *Paediatrics and International Child Health* **38**, S50-  
759 S65 (2018). <https://doi.org:10.1080/20469047.2017.1409454>

760 9 Anderson, J. D. *et al.* Burden of enterotoxigenic Escherichia coli and shigella non-fatal  
761 diarrhoeal infections in 79 low-income and lower middle-income countries: a modelling  
762 analysis. *The Lancet Global Health* **7**, e321-e330 (2019). [https://doi.org:10.1016/s2214-  
763 109x\(18\)30483-2](https://doi.org:10.1016/s2214-109x(18)30483-2)

764 10 Schroeder, G. N. & Hilbi, H. Molecular pathogenesis of Shigella spp.: controlling host cell  
765 signaling, invasion, and death by type III secretion. *Clin Microbiol Rev* **21**, 134-156  
766 (2008). <https://doi.org:10.1128/CMR.00032-07>

767 11 Kotloff, K. L., Riddle, M. S., Platts-Mills, J. A., Pavlinac, P. & Zaidi, A. K. M. Shigellosis. *The*  
768 *Lancet* **391**, 801-812 (2018). [https://doi.org:10.1016/s0140-6736\(17\)33296-8](https://doi.org:10.1016/s0140-6736(17)33296-8)

769 12 Shad, A. A. & Shad, W. A. Shigella sonnei: virulence and antibiotic resistance. *Archives of*  
770 *Microbiology* **203**, 45-58 (2021). <https://doi.org:10.1007/s00203-020-02034-3>

771 13 Network, C. H. A. *Increase in Extensively Drug-Resistant Shigellosis in the United States*,  
772 <https://emergency.cdc.gov/han/2023/han00486.asp> (2023).

- 773 14 Barry, E. M. *et al.* Progress and pitfalls in Shigella vaccine research. *Nature Reviews*  
774 *Gastroenterology & Hepatology* **10**, 245-255 (2013).  
775 <https://doi.org:10.1038/nrgastro.2013.12>
- 776 15 Levine, M. M., Kotloff, K. L., Barry, E. M., Pasetti, M. F. & Sztein, M. B. Clinical trials of  
777 Shigella vaccines: two steps forward and one step back on a long, hard road. *Nature*  
778 *Reviews Microbiology* **5**, 540-553 (2007). <https://doi.org:10.1038/nrmicro1662>
- 779 16 Kaminski, R. W. & Oaks, E. V. Inactivated and subunit vaccines to prevent shigellosis.  
780 *Expert Rev Vaccines* **8**, 1693-1704 (2009). <https://doi.org:10.1586/erv.09.127>
- 781 17 Turbyfill, K. R., Clarkson, K. A., Vortherms, A. R., Oaks, E. V. & Kaminski, R. W. Assembly,  
782 Biochemical Characterization, Immunogenicity, Adjuvanticity, and Efficacy of Shigella  
783 Artificial Invaplex. *mSphere* **3** (2018). <https://doi.org:10.1128/mSphere.00583-17>
- 784 18 Duplessis, C. *et al.* GMP manufacture of Shigella flexneri 2a Artificial Invaplex  
785 (Invaplex(AR)) and evaluation in a Phase 1 Open-label, dose escalating study  
786 administered intranasally to healthy, adult volunteers. *Vaccine* **41**, 6261-6271 (2023).  
787 <https://doi.org:10.1016/j.vaccine.2023.08.051>
- 788 19 Turbyfill, K. R. *et al.* Development of the Shigella flexneri 2a, 3a, 6, and S. sonnei artificial  
789 Invaplex (Invaplex(AR)) vaccines. *mSphere* **8**, e0007323 (2023).  
790 <https://doi.org:10.1128/msphere.00073-23>
- 791 20 Venkatesan, M. M. & Ranallo, R. T. Live-attenuated Shigella vaccines. *Expert Rev*  
792 *Vaccines* **5**, 669-686 (2006). <https://doi.org:10.1586/14760584.5.5.669>
- 793 21 Livio, S. *et al.* Shigella Isolates From the Global Enteric Multicenter Study Inform Vaccine  
794 Development. *Clinical Infectious Diseases* **59**, 933-941 (2014).  
795 <https://doi.org:10.1093/cid/ciu468>
- 796 22 Coster, T. S. *et al.* Vaccination against Shigellosis with Attenuated Shigella flexneri 2a  
797 Strain SC602. *Infection and Immunity* **67**, 3437-3443 (1999).  
798 <https://doi.org:10.1128/iai.67.7.3437-3443.1999>
- 799 23 Barzu, S., Fontaine, A., Sansonetti, P. & Phalipon, A. Induction of a local anti-IpaC  
800 antibody response in mice by use of a Shigella flexneri 2a vaccine candidate:  
801 implications for use of IpaC as a protein carrier. *Infect Immun* **64**, 1190-1196 (1996).  
802 <https://doi.org:10.1128/iai.64.4.1190-1196.1996>
- 803 24 Hartman, A. B. & Venkatesan, M. M. Construction of a stable attenuated Shigella sonnei  
804 DeltavirG vaccine strain, WRSS1, and protective efficacy and immunogenicity in the  
805 guinea pig keratoconjunctivitis model. *Infect Immun* **66**, 4572-4576 (1998).  
806 <https://doi.org:10.1128/IAI.66.9.4572-4576.1998>
- 807 25 Collins, T. A. *et al.* Safety and colonization of two novel VirG(IcsA)-based live Shigella  
808 sonnei vaccine strains in rhesus macaques (*Macaca mulatta*). *Comp Med* **58**, 88-94  
809 (2008).
- 810 26 Barnoy, S. *et al.* Characterization of WRSs2 and WRSs3, new second-generation  
811 virG(icsA)-based Shigella sonnei vaccine candidates with the potential for reduced  
812 reactogenicity. *Vaccine* **28**, 1642-1654 (2010).  
813 <https://doi.org:10.1016/j.vaccine.2009.11.001>
- 814 27 Barnoy, S. *et al.* Shigella sonnei vaccine candidates WRSs2 and WRSs3 are as  
815 immunogenic as WRSS1, a clinically tested vaccine candidate, in a primate model of  
816 infection. *Vaccine* **29**, 6371-6378 (2011). <https://doi.org:10.1016/j.vaccine.2011.04.115>



817 28 Bedford, L. *et al.* Further characterization of *Shigella sonnei* live vaccine candidates  
818 WRSS2 and WRSS3-plasmid composition, invasion assays and Sereny reactions. *Gut*  
819 *Microbes* **2**, 244-251 (2011). <https://doi.org/10.4161/gmic.2.4.17042>

820 29 Ranallo, R. T. *et al.* Two live attenuated *Shigella flexneri* 2a strains WRSf2G12 and  
821 WRSf2G15: A new combination of gene deletions for 2nd generation live attenuated  
822 vaccine candidates. *Vaccine* **30**, 5159-5171 (2012).  
823 <https://doi.org/10.1016/j.vaccine.2012.05.003>

824 30 Jeong, K.-I., Venkatesan, M. M., Barnoy, S. & Tzipori, S. Evaluation of virulent and live  
825 *Shigella sonnei* vaccine candidates in a gnotobiotic piglet model. *Vaccine* **31**, 4039-4046  
826 (2013). <https://doi.org/10.1016/j.vaccine.2013.04.076>

827 31 Ranallo, R. T. *et al.* Oral administration of live *Shigella* vaccine candidates in rhesus  
828 monkeys show no evidence of competition for colonization and immunogenicity  
829 between different serotypes. *Vaccine* **32**, 1754-1760 (2014).  
830 <https://doi.org/10.1016/j.vaccine.2013.12.068>

831 32 Kotloff, K. L. *et al.* Phase I evaluation of delta virG *Shigella sonnei* live, attenuated, oral  
832 vaccine strain WRSS1 in healthy adults. *Infect Immun* **70**, 2016-2021 (2002).  
833 <https://doi.org/10.1128/IAI.70.4.2016-2021.2002>

834 33 Katz, D. E. *et al.* Two Studies Evaluating the Safety and Immunogenicity of a Live,  
835 Attenuated *Shigella flexneri* 2a Vaccine (SC602) and Excretion of Vaccine Organisms in  
836 North American Volunteers. *Infection and Immunity* **72**, 923-930 (2004).  
837 <https://doi.org/10.1128/iai.72.2.923-930.2004>

838 34 Orr, N. *et al.* Community-based safety, immunogenicity, and transmissibility study of the  
839 *Shigella sonnei* WRSS1 vaccine in Israeli volunteers. *Infect Immun* **73**, 8027-8032 (2005).  
840 <https://doi.org/10.1128/IAI.73.12.8027-8032.2005>

841 35 Rahman, K. M. *et al.* Safety, dose, immunogenicity, and transmissibility of an oral live  
842 attenuated *Shigella flexneri* 2a vaccine candidate (SC602) among healthy adults and  
843 school children in Matlab, Bangladesh. *Vaccine* **29**, 1347-1354 (2011).  
844 <https://doi.org/10.1016/j.vaccine.2010.10.035>

845 36 Pitisuttithum, P. *et al.* Clinical Trial of an Oral Live *Shigella sonnei* Vaccine Candidate,  
846 WRSS1, in Thai Adults. *Clinical and Vaccine Immunology* **23**, 564-575 (2016).  
847 <https://doi.org/10.1128/cvi.00665-15>

848 37 Frenck, R. W. *et al.* A Phase I trial to evaluate the safety and immunogenicity of WRSS2  
849 and WRSS3; two live oral candidate vaccines against *Shigella sonnei*. *Vaccine* **36**, 4880-  
850 4889 (2018). <https://doi.org/10.1016/j.vaccine.2018.06.063>

851 38 Raqib, R. *et al.* A phase I trial of WRSS1, a *Shigella sonnei* live oral vaccine in Bangladeshi  
852 adults and children. *Human Vaccines & Immunotherapeutics* **15**, 1326-1337 (2019).  
853 <https://doi.org/10.1080/21645515.2019.1575165>

854 39 Miller, S. I., Ernst, R. K. & Bader, M. W. LPS, TLR4 and infectious disease diversity. *Nature*  
855 *Reviews Microbiology* **3**, 36-46 (2005). <https://doi.org/10.1038/nrmicro1068>

856 40 Chandler, C. E. & Ernst, R. K. Bacterial lipids: powerful modifiers of the innate immune  
857 response. *F1000Research* **6**, 1334 (2017).  
858 <https://doi.org/10.12688/f1000research.11388.1>

859 41 Zamyatina, A. & Heine, H. Lipopolysaccharide Recognition in the Crossroads of TLR4 and  
860 Caspase-4/11 Mediated Inflammatory Pathways. *Front Immunol* **11**, 585146 (2020).  
861 <https://doi.org:10.3389/fimmu.2020.585146>

862 42 Scott, A. J., Oyler, B. L., Goodlett, D. R. & Ernst, R. K. Lipid A structural modifications in  
863 extreme conditions and identification of unique modifying enzymes to define the Toll-  
864 like receptor 4 structure-activity relationship. *Biochimica et Biophysica Acta (BBA) -  
865 Molecular and Cell Biology of Lipids* **1862**, 1439-1450 (2017).  
866 <https://doi.org:10.1016/j.bbalip.2017.01.004>

867 43 Park, B. S. *et al.* The structural basis of lipopolysaccharide recognition by the TLR4–MD-2  
868 complex. *Nature* **458**, 1191-1195 (2009). <https://doi.org:10.1038/nature07830>

869 44 Raetz, C. R. H., Reynolds, C. M., Trent, M. S. & Bishop, R. E. Lipid A Modification Systems  
870 in Gram-Negative Bacteria. *Annual Review of Biochemistry* **76**, 295-329 (2007).  
871 <https://doi.org:10.1146/annurev.biochem.76.010307.145803>

872 45 Simpson, B. W. & Trent, M. S. Pushing the envelope: LPS modifications and their  
873 consequences. *Nature Reviews Microbiology* **17**, 403-416 (2019).  
874 <https://doi.org:10.1038/s41579-019-0201-x>

875 46 Rossi, O. *et al.* Modulation of Endotoxicity of Shigella Generalized Modules for  
876 Membrane Antigens (GMMA) by Genetic Lipid A Modifications. *Journal of Biological  
877 Chemistry* **289**, 24922-24935 (2014). <https://doi.org:10.1074/jbc.m114.566570>

878 47 Ernst, R. K., Pelletier, M. & Hajjar, A. Immunotherapeutic potential of modified  
879 lipooligosaccharides/lipid a. United States patent US20160002691A1.

880 48 Yang, H. *et al.* Lipid A Structural Determination from a Single Colony. *Anal Chem* **94**,  
881 7460-7465 (2022). <https://doi.org:10.1021/acs.analchem.1c05394>

882 49 MacLennan, C. A., Grow, S., Ma, L. F. & Steele, A. D. The Shigella Vaccines Pipeline.  
883 *Vaccines (Basel)* **10** (2022). <https://doi.org:10.3390/vaccines10091376>

884 50 Gregg, K. A. *et al.* Rationally Designed TLR4 Ligands for Vaccine Adjuvant Discovery.  
885 *mBio* **8**, e00492-00417 (2017). <https://doi.org:10.1128/mbio.00492-17>

886 51 Gregg, K. A. *et al.* A lipid A-based TLR4 mimetic effectively adjuvants a Yersinia pestis rF-  
887 V1 subunit vaccine in a murine challenge model. *Vaccine* **36**, 4023-4031 (2018).  
888 <https://doi.org:10.1016/j.vaccine.2018.05.101>

889 52 Haupt, R. E. *et al.* Novel TLR4 adjuvant elicits protection against homologous and  
890 heterologous Influenza A infection. *Vaccine* **39**, 5205-5213 (2021).  
891 <https://doi.org:10.1016/j.vaccine.2021.06.085>

892 53 Zacharia, A. *et al.* Optimization of RG1-VLP vaccine performance in mice with novel TLR4  
893 agonists. *Vaccine* **39**, 292-302 (2021). <https://doi.org:10.1016/j.vaccine.2020.11.066>

894 54 Alexander-Floyd, J. *et al.* Position-Specific Secondary Acylation Determines Detection of  
895 Lipid A by Murine TLR4 and Caspase-11. *Infect Immun* **90**, e0020122 (2022).  
896 <https://doi.org:10.1128/iai.00201-22>

897 55 Harberts, E. M. *et al.* Lipid A Variants Activate Human TLR4 and the Noncanonical  
898 Inflammasome Differently and Require the Core Oligosaccharide for Inflammasome  
899 Activation. *Infect Immun* **90**, e0020822 (2022). <https://doi.org:10.1128/iai.00208-22>

900 56 Haupt, R. *et al.* Enhancing the protection of influenza virus vaccines with BECC TLR4  
901 adjuvant in aged mice. *Sci Rep* **13**, 715 (2023). [https://doi.org:10.1038/s41598-023-  
902 27965-x](https://doi.org:10.1038/s41598-023-27965-x)

903 57 Pettengill, M. *et al.* Human alkaline phosphatase dephosphorylates microbial products  
904 and is elevated in preterm neonates with a history of late-onset sepsis. *PLoS One* **12**,  
905 e0175936 (2017). <https://doi.org:10.1371/journal.pone.0175936>

906 58 D’Hauteville, H. L. N. *et al.* Two msbB Genes Encoding Maximal Acylation of Lipid A Are  
907 Required for Invasive *Shigella flexneri* to Mediate Inflammatory Rupture and Destruction  
908 of the Intestinal Epithelium. *The Journal of Immunology* **168**, 5240-5251 (2002).  
909 <https://doi.org:10.4049/jimmunol.168.10.5240>

910 59 Ranallo, R. T. *et al.* Virulence, inflammatory potential, and adaptive immunity induced  
911 by *Shigella flexneri* msbB mutants. *Infect Immun* **78**, 400-412 (2010).  
912 <https://doi.org:10.1128/IAI.00533-09>

913 60 Carty, S. M., Sreekumar, K. R. & Raetz, C. R. Effect of cold shock on lipid A biosynthesis in  
914 *Escherichia coli*. Induction At 12 degrees C of an acyltransferase specific for  
915 palmitoleoyl-acyl carrier protein. *J Biol Chem* **274**, 9677-9685 (1999).  
916 <https://doi.org:10.1074/jbc.274.14.9677>

917 61 Needham, B. D. & Trent, M. S. Fortifying the barrier: the impact of lipid A remodelling on  
918 bacterial pathogenesis. *Nat Rev Microbiol* **11**, 467-481 (2013).  
919 <https://doi.org:10.1038/nrmicro3047>

920 62 Sambrook, J. & Green, M. R. *Molecular cloning : a laboratory manual*. (Cold Spring  
921 Harbor Laboratory Press, 2001).

922 63 Stokes, M. G. *et al.* Oral administration of a *Salmonella enterica*-based vaccine  
923 expressing *Bacillus anthracis* protective antigen confers protection against aerosolized  
924 *B. anthracis*. *Infect Immun* **75**, 1827-1834 (2007). <https://doi.org:10.1128/IAI.01242-06>

925 64 McKenzie, G. J. & Craig, N. L. Fast, easy and efficient: Site-specific insertion of  
926 transgenes into Enterobacterial chromosomes using Tn7 without need for selection of  
927 the insertion event. *BMC Microbiology* **6**, 39 (2006). [https://doi.org:10.1186/1471-2180-](https://doi.org:10.1186/1471-2180-6-39)  
928 [6-39](https://doi.org:10.1186/1471-2180-6-39)

929 65 Aziz, R. K. *et al.* The RAST Server: rapid annotations using subsystems technology. *BMC*  
930 *Genomics* **9**, 75 (2008). <https://doi.org:10.1186/1471-2164-9-75>

931 66 Sorensen, M. *et al.* Rapid microbial identification and colistin resistance detection via  
932 MALDI-TOF MS using a novel on-target extraction of membrane lipids. *Scientific Reports*  
933 **10** (2020). <https://doi.org:10.1038/s41598-020-78401-3>

934 67 Niedermeyer, T. H. J. & Strohal, M. mMass as a Software Tool for the Annotation of  
935 Cyclic Peptide Tandem Mass Spectra. *PLoS ONE* **7**, e44913 (2012).  
936 <https://doi.org:10.1371/journal.pone.0044913>

937 68 Folch, J., Lees, M. & Sloane Stanley, G. H. A simple method for the isolation and  
938 purification of total lipides from animal tissues. *J Biol Chem* **226**, 497-509 (1957).

939 69 Hirschfeld, M., Ma, Y., Weis, J. H., Vogel, S. N. & Weis, J. J. Cutting Edge: Repurification  
940 of Lipopolysaccharide Eliminates Signaling Through Both Human and Murine Toll-Like  
941 Receptor 2. *The Journal of Immunology* **165**, 618-622 (2000).  
942 <https://doi.org:10.4049/jimmunol.165.2.618>

943

# Figures

Figure 1

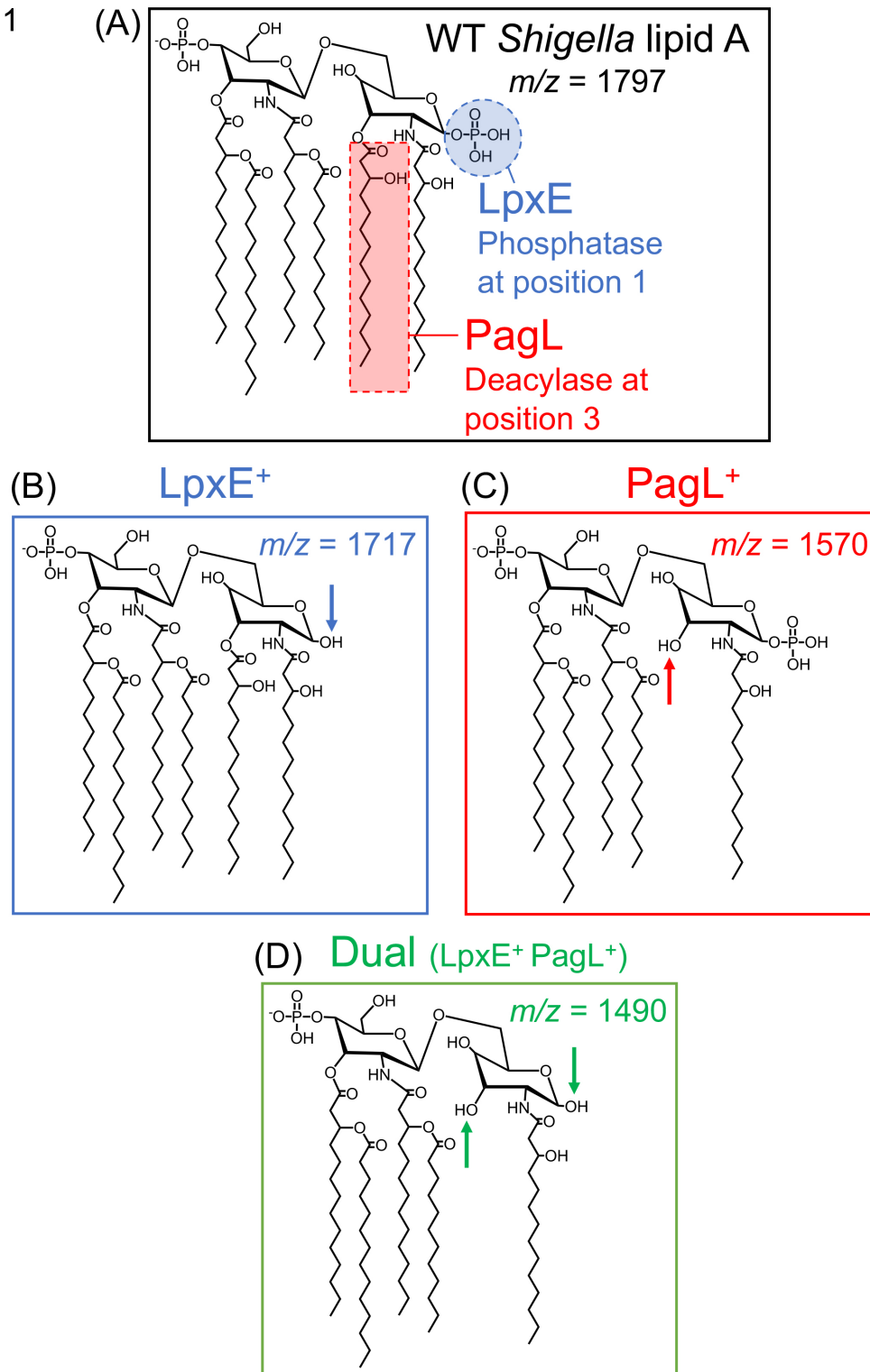


Figure 1

Lipid A modifications generated by BECC constructs used in this study

(A) The WT lipid A structure of *Shigella* along with the (B) LpxE- (C) PagL- and (D) Dual-modified resultant structures, lacking a phosphate, 3OH C14 acyl chain, or both, respectively. The expected  $m/z$  for the  $[M-H]^-$  ions observed in MALDI-TOF spectra are displayed for each structure.

Figure 2

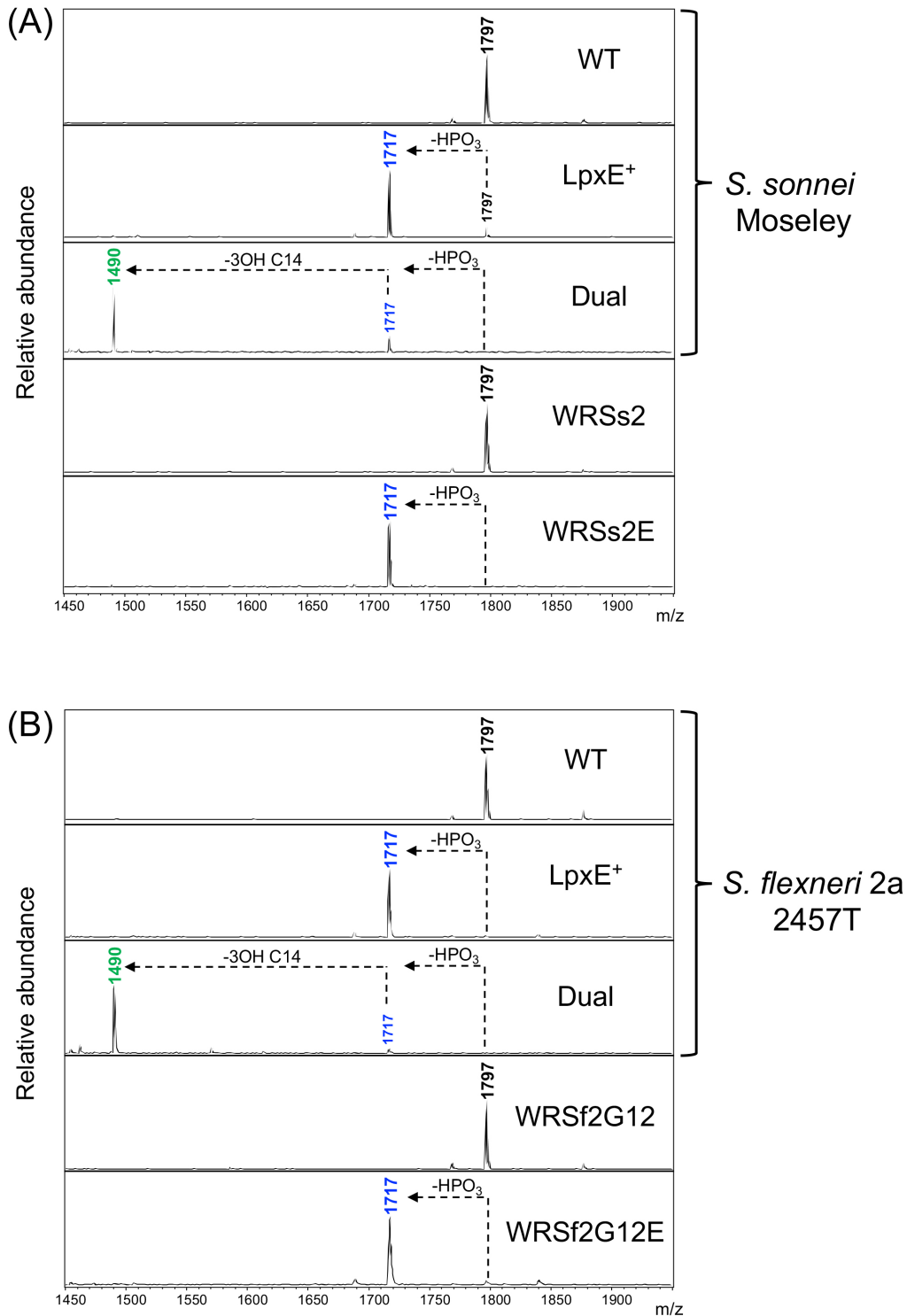


Figure 2

**MALDI-TOF MS analysis of lipid A related peaks for BECC-modified *Shigella* strains** Representative MALDI-TOF MS spectra for WT and vaccine strains of (A) *S. sonnei* and (B) *S. flexneri* 2a chromosomally

expressing *lpxE* or Dual. Spectral peaks represent  $[M-H]^+$  ions. Colored peaks correspond to the expected structures detailed in Figure 1. Arrows depict the loss of a phosphate ( $HPO_3$ ) or acyl chain ( $3OH\ C14$ ) from the indicated lipid A species.

Figure 3

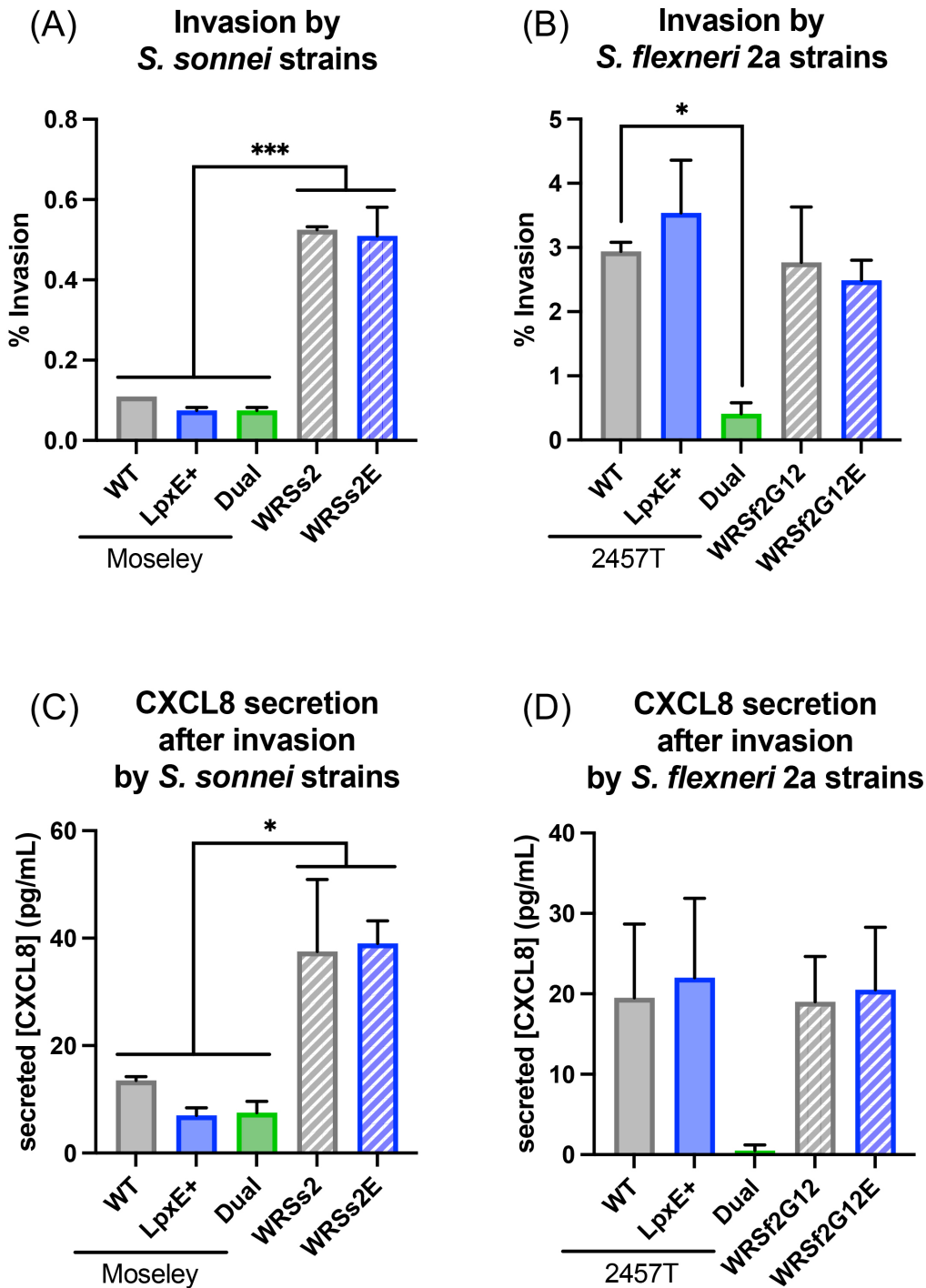


Figure 3

Invasion of epithelial cells by *Shigella* and corresponding CXCL8 production

Invasion of HT29 cells after 4 hours of infection (MOI of 10) with (A) *S. sonnei* and (B) *S. flexneri* 2a strains. CXCL8 production in the cell supernatant after the 4-hour infection with (C) *S. sonnei* and (D) *S. flexneri* 2a strains. Statistical significance determined by ordinary one-way ANOVA. \* and \*\*\* represent p-values of < 0.05 and < 0.001, respectively.

Figure 4

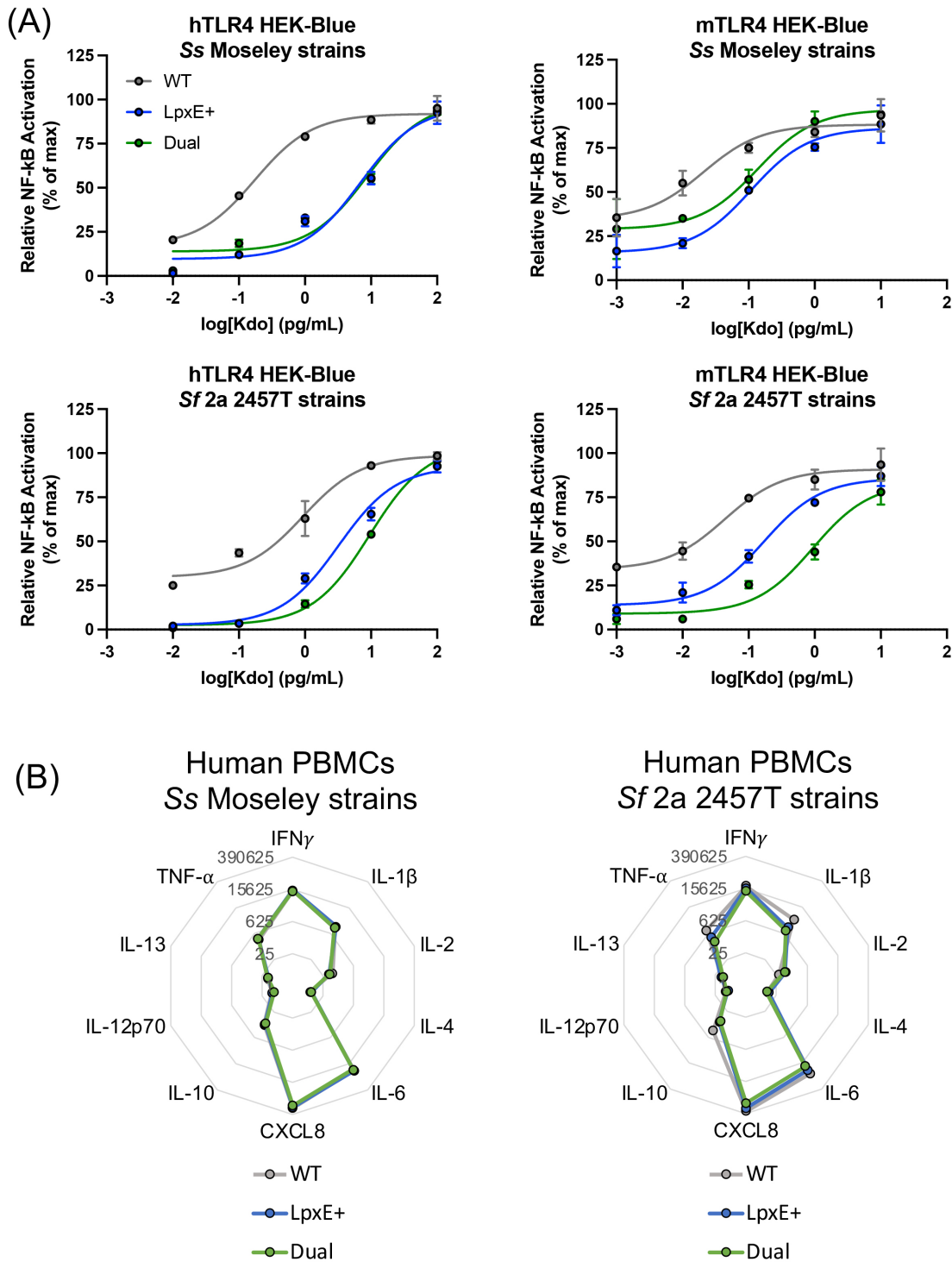


Figure 4

**Stimulation of reporter and primary cells with Kdo normalized LPS from *Shigella*** (A) HEK-Blue cells stably expressing an NF- $\kappa$ B reporter under the control of the human and mouse orthologs of TLR4/MD-2/CD-14 (named hTLR4 or mTLR4, respectively) were stimulated across 10-fold dilutions, in duplicate, of Kdo standardized LPS for 18 hours at 37°C with 5% CO<sub>2</sub>. LPS was purified from *S. sonnei* Moseley or *S. flexneri* 2a 2457T. (B) Representative cytokine profile from one PBMC donor, as measured by MSD multiplex, upon stimulation of the PBMCs with the aforementioned LPS at 1 pg/mL Kdo for 48 hours at 37°C with 5% CO<sub>2</sub>. Numbers in grey denote cytokine concentration in pg/mL.

Figure 5

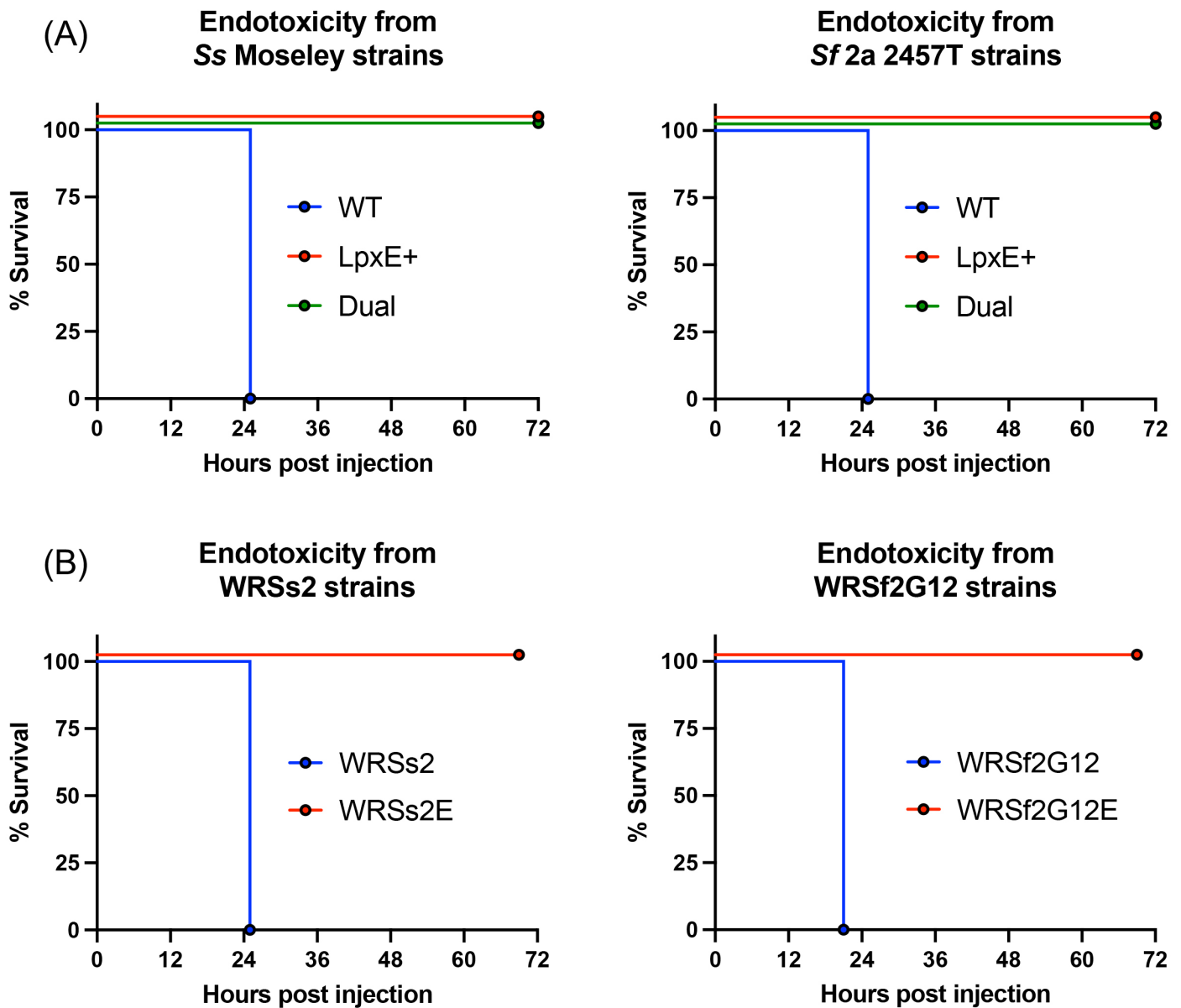


Figure 5

**Assessment of the toxicity of *Shigella* LPS via a murine acute endotoxemia model** Survival curves for mice (n=5) receiving a Kdo normalized dose of LPS intraperitoneally, representative of 15 mg/kg, using



purified LPS from (A) WT strains and (B) vaccine strains of *S. sonnei* and *S. flexneri* 2a.

Figure 6

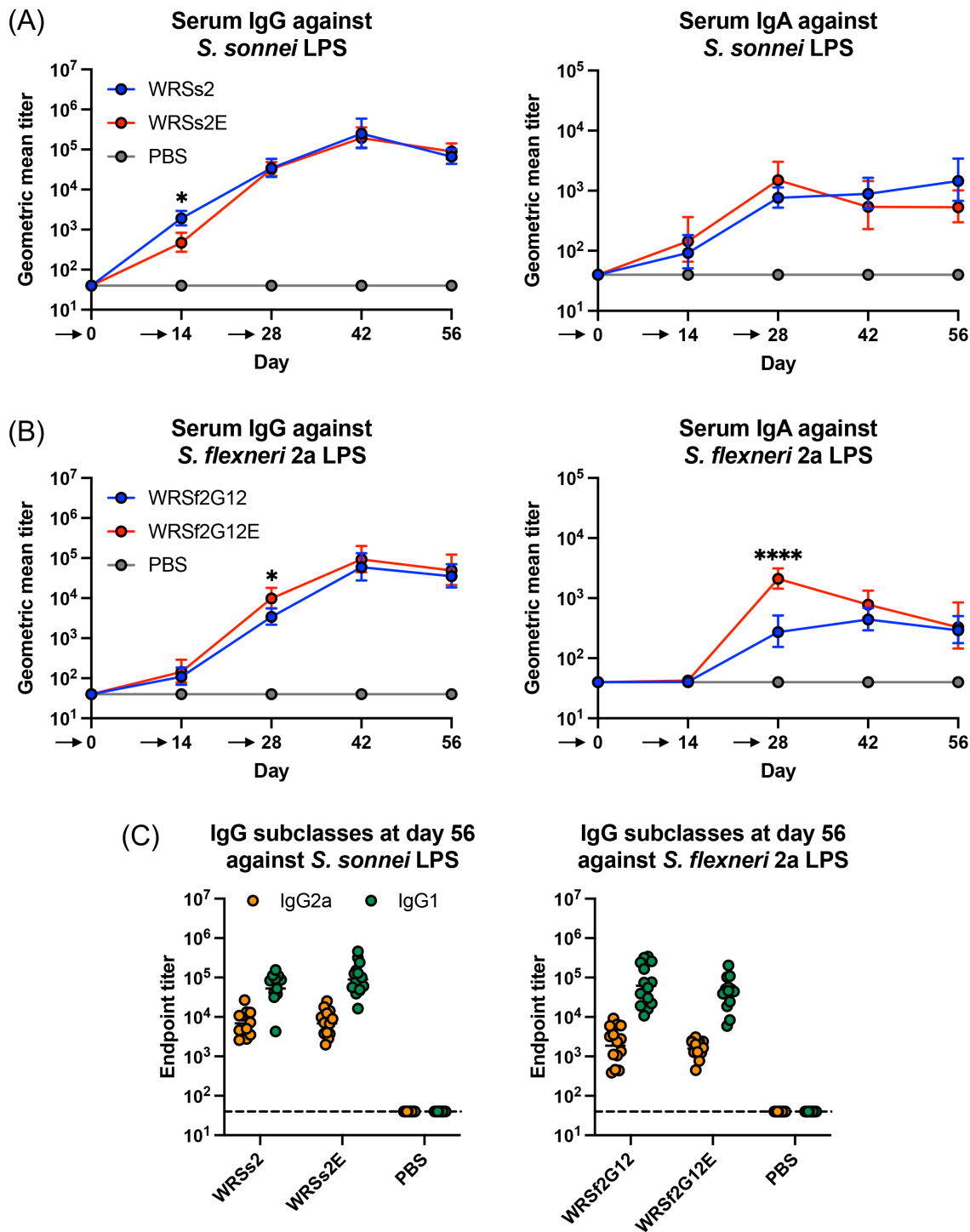


Figure 6

### Antibody titers from a *Shigella* murine vaccine study

Serum IgG and IgA geometric mean titers against (A) *S. sonnei* Moseley LPS or (B) *S. flexneri* 2a 2457T LPS for mice (n=15) vaccinated intranasally with 10<sup>6</sup> CFU at day 0, 14, and 28 as indicated by the arrows

below the X-axis. (C) Serum IgG2a and IgG1 titers at day 56 against serotype-specific LPS. Statistical significance was determined by 2way ANOVA. \* and \*\*\*\* represent p-values of  $< 0.05$  and  $< 0.0001$ , respectively.

## Supplementary Files

This is a list of supplementary files associated with this preprint. Click to download.

- [Supplemental.pdf](#)